Journal of Pharmaceutical Innovation (2019) 14:259–285
https://doi.org/10.1007/s12247-018-9347-8

ORIGINAL ARTICLE

Combined Feedforward/Feedback Control of an Integrated Continuous Granulation Process

Glinka Cathy Pereira[1] · Shashank Venkat Muddu[1] · Andrés David Román-Ospino[1] · Don Clancy[2] · Benoit Igne[2] · Christian Airiau[2] · Fernando J. Muzzio[1] · Marianthi Ierapetritou[1] · Rohit Ramachandran[1] · Ravendra Singh[1]

Published online: 4 October 2018

Abstract

Purpose Continuous manufacturing offers shorter processing times and increased product quality assurance, among several other advantages. This makes it an ever-growing interest among pharmaceutical companies. A suitable efficient control system is however desired for continuous pharmaceutical manufacturing to achieve a consistent predefined end product quality.

Methods In order to control product quality more accurately, the effects of input disturbances need to be proactively mitigated. Therefore, it is desired that a combined feedforward/feedback control system integrated with suitable process analytical technology (PAT) be implemented over a traditional feedback-only control system. The feedforward controller measures and takes corrective actions for disturbances proactively before they affect the process and thereby product quality. The feedback controller considers the real-time deviation of control variable from a pre-specified set point and keeps it at a minimum possible value. The deviation of a control variable from the set point could be due to both measurable and unmeasurable disturbances.

Results In this work, a combined control strategy has been developed for a continuous twin screw wet granulation (WG) process. An integrated flowsheet model was developed and simulated in order to evaluate the effect of control loops on critical quality attributes (CQAs). Different strategies of manipulation were evaluated and the best strategy was identified.

Conclusions In silico study on the combined feedforward/feedback control strategy and feedback-only control strategy demonstrates that the combined loop results in diminished variability of the CQAs.

Keywords Continuous pharmaceutical manufacturing · Feedforward control · Feedback control · Continuous twin screw granulator (TSG) · Process analytical technology

Introduction

Continuous manufacturing has been in use for a long time in the petrochemical, metal casting, and bulk chemical industries. However, it has recently been of growing interest in the pharmaceutical sector because it offers substantial economic benefits along with increased product quality assurance among several other advantages [1]. In 2002, the FDA launched an initiative that supports a risk-based approach towards modernizing pharmaceutical manufacturing. In December 2015, the agency also published a draft guidance which encourages the industry to move towards continuous manufacturing aligned with quality by design (QbD) [2, 3]. In the past decade, extensive work has been carried out to study the benefits of continuous pharmaceutical manufacturing over batch-wise manufacturing. Studies have also been carried out as to how academia, industry, and regulatory bodies can work together to promote development of continuous manufacturing for the development of small molecules [4].

Product quality in pharmaceutical drug manufacturing, one of the most strictly regulated manufacturing practices, is of utmost importance. Variations in the properties of raw materials and process disturbances affect the quality of the product. These variations are a result of factors such as noise from the various unit operations, process conditions, and variations in raw materials. The development of an advanced control strategy is useful for adhering to the stringent quality criteria.

✉ Ravendra Singh
ravendra.singh@rutgers.edu

[1] Engineering Research Center for Structured Organic Particulate Systems (C-SOPS), Department of Chemical and Biochemical Engineering, Rutgers, The State University of New Jersey, Piscataway, NJ 08854, USA

[2] Glaxo Smith Kline (GSK), King of Prussia, PA 19406, USA

Since the initiative by the FDA on continuous manufacturing came into existence, a large amount of research has been carried out to study the role of control systems in pharmaceutical drug manufacturing. Muteki et al. suggested a feedforward control strategy for a dry granulation process using a partial least squares model to compensate for the effect of variability in raw materials on the final tablet properties [5]. A detailed study has been carried out in developing control strategies for different continuous granulators such as high shear granulator and fluid bed granulator [6–8]. Singh et al. have designed and implemented a hybrid model predictive control (MPC) system and a simple proportional integral derivative (PID) control system on a pilot-scale direct compaction continuous tablet manufacturing process [9]. A combined feedforward/feedback control system for an integrated continuous direct compaction tablet manufacturing process has been also developed [10]. A feedback control system for a twin screw granulator (TSG) with focus on controlling granule properties has been also proposed [11]. However, no attempt has been made to design an advanced feedforward/feedback control system for an integrated continuous tablet manufacturing process via wet granulation that can enable drug concentration control.

Traditional feedback controllers are essential in a control loop to ensure product quality. These controllers take action only after the disturbance has propagated through the system and affected the product quality. On the other hand, a feedforward only controller takes action before the disturbance propagates. However, it does not take into account the real-time measurement of control variables and cannot assure product quality. Therefore, it is desired that a combined feedforward/feedback control system integrated with suitable process analytical technology (PAT) be implemented over a traditional feedback control system. The feedforward controller measures and takes corrective actions for disturbances before they affect the process while the feedback controller considers the effect of process parameters and ensures the consistency of the output.

As mentioned above, since the FDA's initiative in 2002 for modernizing pharmaceutical manufacturing, efforts were made towards continuous manufacturing and implementation of control systems with suitable PAT. A guidance for industry PAT was published by the FDA in 2004 to encourage industry to improve the production process [12]. For continuous manufacturing, it is necessary to analyze data continuously in real time, to take specific control actions in order to ensure product quality. This is where the bridge between PAT and control systems is established. One of the PAT techniques in the pharmaceutical industry used to analyze different critical quality attributes (CQAs) is the near infrared (NIR) spectroscopy. Vanarase et al. applied NIR for the monitoring of drug concentration into a continuous blending process [13]. Singh et al. implemented a hybrid MPC-PID control for continuous tablet manufacturing with real-time monitoring of API composition using NIR at the outlet of a continuous blender [14]. A method for real-time monitoring of powder bulk density needed for combined feedforward/feedback control of a continuous direct compaction manufacturing process has also been developed [15].

In this work, an advanced control system has been designed for an integrated continuous pharmaceutical tablet manufacturing process via wet granulation. The considered process consists of two feeders and one twin screw granulator. Different control architectures were developed, evaluated, and compared in order to identify the best control strategy. A feedback-only control strategy has been compared with a combined feedforward/feedback control strategy. The methods for real-time monitoring of control variables were also developed. The control system has been designed, integrated, and implemented in gPROMS (Process Systems Enterprise) and Simulink (The Mathworks, Natick, MA, USA) with mathematical models for all unit operations to evaluate the performance.

Integrated Continuous Granulation Process

Granulation is a size enlargement process that improves flow and handling and increases uniformity in the end product. There are three tablet manufacturing routes, wet granulation, dry granulation, and direct compaction. This work only focusses on wet granulation. This process involves the addition of a liquid binder to a powder bed where it undergoes wetting, nucleation, consolidation, growth, breakage, and attrition simultaneously. With industries and regulatory bodies focusing on continuous manufacturing, continuous wet granulation is an active area for research. Since granulation largely affects homogeneity of the active ingredient in the bulk product, it is very important to control this unit operation. Major variations in the process are due to variations in raw materials and perturbations from the feeders, hence controlling at this stage is important in order to avoid further variations in downstream processes that are difficult to control.

Process Description

The process section considered for this study is shown in Fig. 1. This section is part of an integrated continuous pharmaceutical tablet manufacturing process via wet granulation route. In this wet granulation process, two gravimetric feeders have been integrated with a continuous twin screw granulator (TSG) (ThermoFisherScientific, Waltham, MA, USA). The process involves a batch pre-blending step where the API and intragranular components are mixed and subsequently fed into feeder 1. The blend consists of 12% API and 88% excipients. The other feeder, feeder 2 is for excipients only.

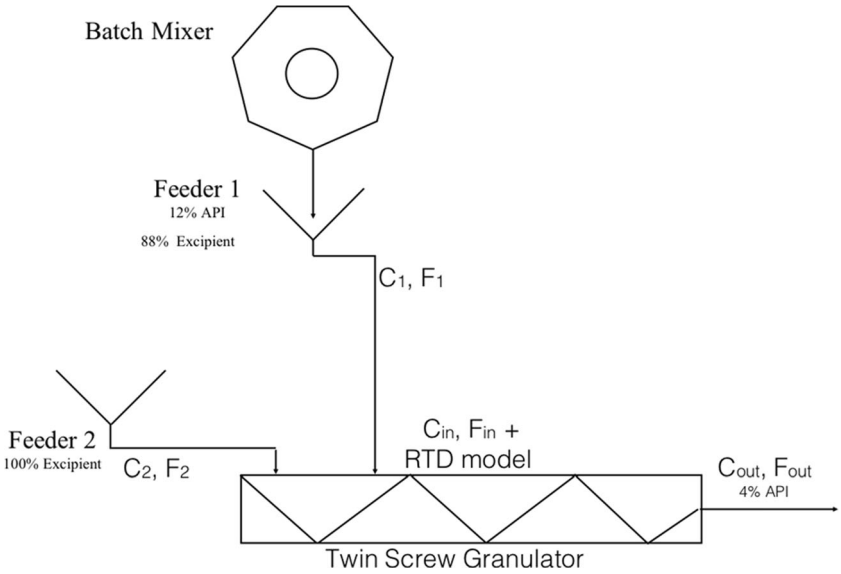

Fig. 1 Integrated continuous wet granulation process flowsheet without control loops

The K-Tron gravimetric feeders are the loss-in-weight feeders. They consist of a hopper and a twin screw that conveys dry bulk material out of the feeder at a constant weight per unit time and adjusts the screw speed to control flow rate.

The TSG is integrated after the two feeder hoppers where the streams are mixed and passed with a specific liquid to solid (L/S) ratio to form granules. The feed from the two streams enters the TSG in the transport zone. The liquid binder used for the granulation process is water which is added before the first kneading block. The powder then passes into the mixing zone where it is wetted and forms granules that are conveyed further down by the twin screws. The comingling of the two feeder streams leads to an overall low concentration of API at the granulator outlet. The granule product is then dried, milled, and batch blended with superdisintegrants and extragranular excipients (to further dilute API to ~1%), and then compressed and coated. Currently, a potential source of product variability is the lack of homogeneity of the stream entering the granulator. The noise propagated by the screws of the feeder to the powder being fed also causes a change in the concentration of API. Pre-blends discharged by a tumbling blender are known to fluctuate fairly significantly in composition and due to limited back mixing in the TSG, these fluctuations are propagated to the granulator exit, affecting the content uniformity of API in the granules. In turn, such variability can affect both product content uniformity (CU) and product dissolution characteristics. Fortunately, since the composition of the stream discharged by the feeder can be assayed instantaneously using PAT methods, it is conceptually possible to adjust the ratio of the API-bearing stream and the excipient-only stream, and their flow rates, to compensate for composition fluctuations entering, and therefore exiting, the granulator.

Integrated Process Flowsheet Model

Unit Operations Model

In order to implement continuous manufacturing, various models were built for the different unit operations involved in the continuous tablet manufacturing process via wet granulation to enhance in silico study. These models were developed in the gPROMS library to facilitate integrated flowsheet modeling. The procedure for dynamic flowsheet modeling of continuous pharmaceutical manufacturing using individual models and integrating them together has been previously reported [16–18].

Feeder

The feeders are used to provide the stream containing the preblend of API and excipient and the stream containing only excipients to the process. The process model used for this integrated flowsheet simulation and control has been previously developed [19]. This model is based on the Heckel model that relates powder density to its pressure thus effectively developing the feed factor model for the feeder.

Continuous Granulation (TSG)

A twin screw granulator consists of two parallel screws in the barrel, with each screw having its own mixing, kneading, and conveying elements. The conveying elements transport the material along the length of the granulator. The mixing and kneading elements provide the back mixing required to produce granules/blends of homogeneous composition. While performing granulation experiments, it is also observed that

some material deposits on the walls of the barrel and on the screws. Residence time distribution (RTD) modeling for the twin screw granulator can be achieved using three conceptual models. A tanks-in-series (TIS) model without plug flow volume fraction, a TIS model with plug flow volume fraction, and a TIS model with plug flow volume fraction and dead zones. The comparison between these three conceptual models has been previously reported and it was suggested that the TIS model with plug flow volume fraction and dead zones simulated the experimental RTD best [20].

Therefore, in this work, the twin screw granulator was modeled akin to a reactor system as the material flows through the granulator like a plug flow shown in Fig. 2. However, to account for the back mixing provided by the mixing and kneading elements, the model developed consists of continuously stirred tank reactor (CSTR) elements too. Lastly, the material that remains in the granulator was incorporated as dead volume fraction. It has been assumed that the dead volume fraction is small enough so that the volumetric amount of material exiting the system is approximately the same as the material fed in the unit operation.

As shown in Fig. 2, the proposed model consists of two streams, where each stream consists of a plug flow reactor (PFR) in series with finite number of CSTRs with their own accompanying dead volumes. For simplicity, it was assumed that no cross flow occurs between the two streams and that the dead volumes of the CSTRs in any one stream are equivalent for all the CSTRs in that split.

The pulse tracer RTD response function $E(t)$ for a system of two parallel streams of PFR and CSTRs with dead volumes in series is given by Eq. 1.

$$E(\theta) = t_m E(t) = \frac{f}{(n-1)!}(b\beta)^n(\theta-p)^{n-1}\exp\left(-b\beta(\theta-p)\right) + \frac{1-f}{(m-1)!}\left(\frac{g\beta}{\alpha}\right)^m(\theta-q)^{m-1}\exp\left(-\frac{g\beta}{\alpha}(\theta-q)\right) \quad (1)$$

where

$$\theta = \frac{t}{t_m}$$

$$b = \frac{n}{(1-p)(1-d)}$$

$$g = \frac{m}{(1-q)(1-h)}$$

$$\beta = f + (1-f)\alpha$$

Where n is the number of CSTRs in stream 1, m is the number of CSTRs in stream 2, (n is not necessarily equal to m), t is the time, t_m is the mean residence time (MRT) of the system, θ is the dimensionless time with respect to the mean residence time of the entire system, f is the fraction of material going into the first stream, α is the ratio of MRT in stream 2 to MRT in stream 1, p is the fraction of PFR (volume basis) of stream 1, q is the fraction of PFR (volume basis) of stream 2, d is the fraction of dead region (volume basis) of stream 1, and h is the fraction of dead region (volume basis) of stream 2.

The model parameters must be fit for each experimental run. For the same purpose, pulse tracer experiments should be carried out and the normalized exit age function of the tracer must be obtained. The model is then fitted to the experimental data by minimizing the sum of squared errors (SSE) between the model prediction values and the experimental data. A model curve showing the fitting of TSG RTD experimental data as a function of time is shown in Fig. 3. Here, the experimental data generated was fitted to the model through an optimization algorithm in MATLAB. From the initial guess parameters, the final parameters were obtained by minimizing the SSE between the experimental $E(t)$ values and the model $E(t)$ values. The blue dashed line in the figure represents the $E(t)$ values calculated from the initial guess of parameters. The red dashed line indicates the optimized $E(t)$ values and the pink dots represent the experimental data.

The step change response function $F(\theta)$ for the same system model, i.e., two streams with each having plug flow

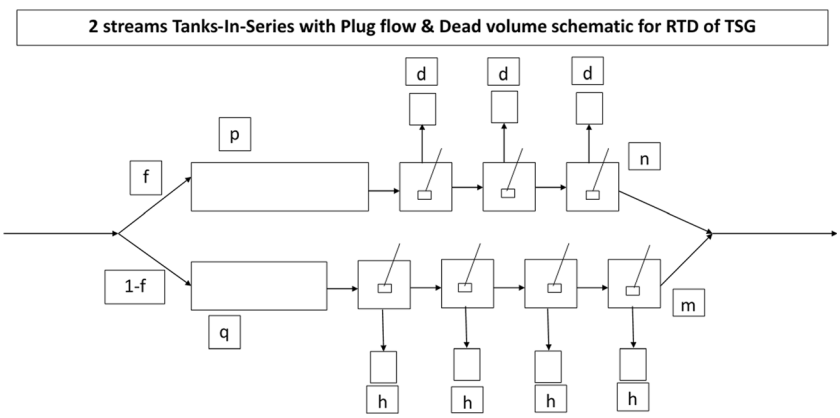

Fig. 2 Tank-in-series with plug flow fraction and dead volume schematic for RTD of twin screw granulator

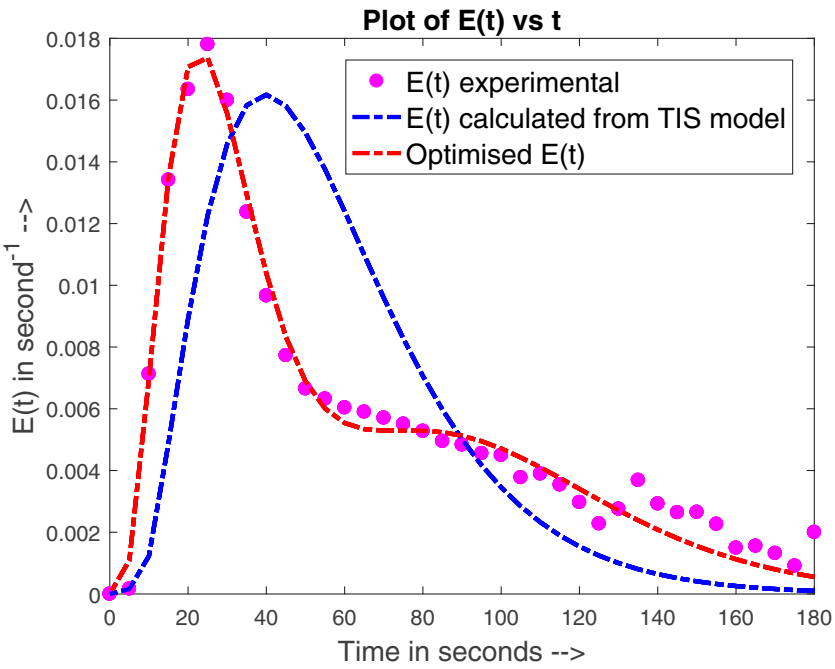

Fig. 3 Optimized $E(t)$ data and its fit to experimental data

fraction and finite number of CSTRS with dead volume fractions is given by Eqs. 2, 3, and 4.

$$F(\theta) = \frac{f}{(n-1)!}\left(\Gamma(n) - \Gamma(n, b\beta(\theta - p))\right) + \frac{(1-f)}{(m-1)!}\left(\Gamma(m) - \Gamma\left(m, \frac{g\beta}{\alpha}(\theta - q)\right)\right) \quad (2)$$

$$F(\theta) = \int_0^\infty E(\theta)\, d\theta = \int_p^\infty E_1(\theta)\, d\theta + \int_q^\infty E_2(\theta)\, d\theta \quad (3)$$

$$E(\theta) = t_m E(t) \quad (4)$$

where

$$\theta = \frac{t}{t_m}$$

$$b = \frac{n}{(1-p)(1-d)}$$

$$g = \frac{m}{(1-q)(1-h)}$$

From this, the outlet concentration at the exit of the granulator is given by Eq. 5.

$$C(t) = C_0 F(\theta) \quad (5)$$

where C_0 is the inlet stream concentration of the monitored species. A model curve showing the response to a step change in the input concentration of the material, as a function of time is shown in Fig. 4. The response to a step change in the system was simulated in the gPROMS Model Builder software. A step change from 4% concentration to 5% concentration of API was made. As seen in the figure, the RTD model implemented in gPROMS predicts the expected concentration (0.05) at the exit of the granulator.

Integration of the Unit Operations Model

The feeder model and the granulator model discussed in the "Unit Operations Model" Section were then used to facilitate integrated flowsheet modeling in gPROMS as shown in Fig. 5. Each of the feeders has a PID controller that controls the outlet flow rate of the feeder. Outlet from the feeders (flow rate and concentration) is passed on to the granulator as two different streams. Stream 1 connects the API feeder to the

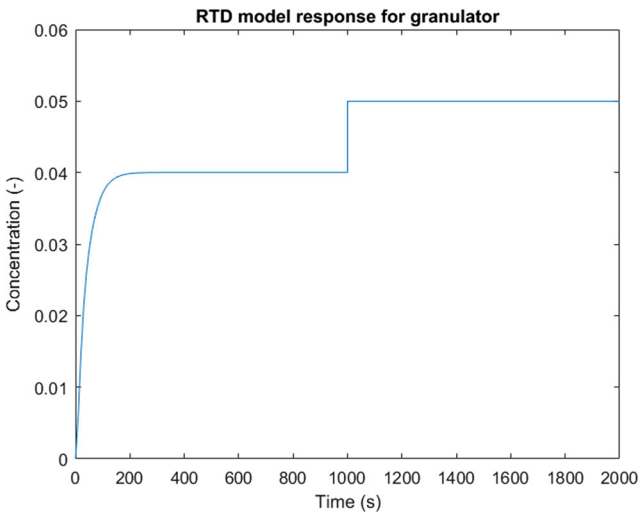

Fig. 4 RTD response to a step change in input concentration of any unit operation (gPROMS)

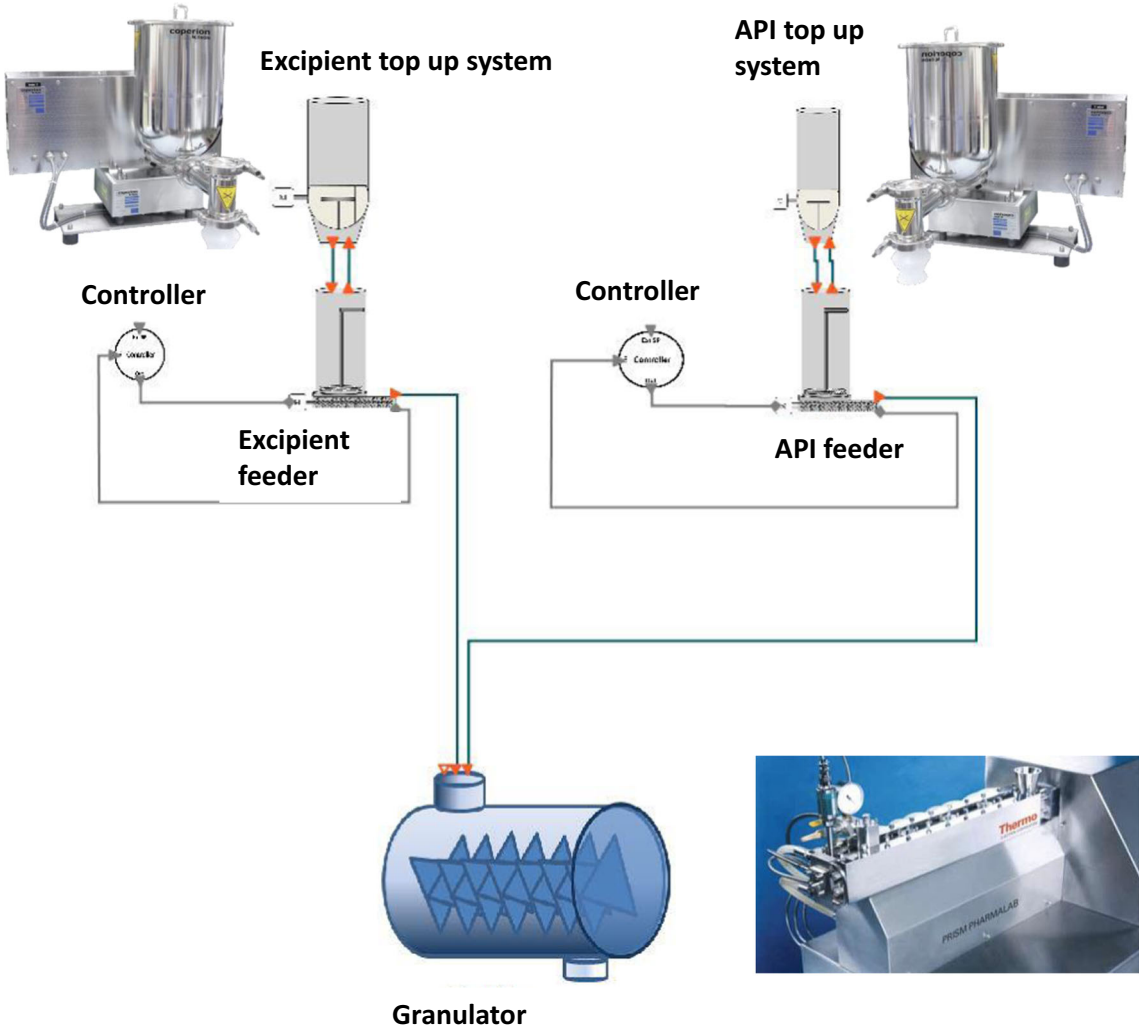

Fig. 5 Integrated flowsheet model (open loop)

granulator. Concentration of API in this stream is ideally 12%. Stream 2 connects excipient feeder to the granulator. There should be no API in this stream. The PID controller maintains the flow rate of the feeder at the desired set point. The measured variable for these PID controllers is the flow rate coming out of the feeder and the manipulated variable is the screw rotational speed. The variables important for the design of the control system have been discussed in detail in the "Results and Discussion" Section.

Table 1 Different control options based on actuator

Type of actuation	Actuator	Controlled variable	Advantages	Disadvantages
Non-linear	Flow rate set point of excipient feeder	API composition in granules	Input disturbances in API composition are lesser since only one feeder flow rate is actuating	Only API composition in granules is controlled and not the total flow rate. Nonlinear actuator has restrictions with implementing MPC since either a nonlinear MPC would have to be developed or the actuator needs to be linearized.
Linear	API ratio set point	API composition in granules	Production rate is controlled along with API composition in granules. Easier to implement an MPC controller for a linear actuator	Input disturbances in API composition are introduced due to changes in API feeder flow rate.

Identification of Control Loops

There are different options to control the concentration of API in granules at the granulator outlet. In order to control this variable, the API composition at the inlet of the granulator needs to be manipulated which can be achieved in two ways. Based on the variable to be actuated, the two different options to control composition of API are listed in Table 1. As given in the table, there are two possible actuator candidates to control the composition of API in granules. The first actuator is the flow rate of the excipient feeder. In this option, keeping the flow rate of API feeder constant, the flow rate of the excipient feeder can be manipulated. The second option is that of actuating the API Ratio. The API ratio is a ratio that results from the material balance given in Eq. 6 and is represented in Eq. 7. Actuating the API ratio leads to maintaining a consistent API composition. In this case, the total flow rate is also kept constant which is the summation of flow rates of the two feeders. Thus, from Eq. 2, the set point for flow rate of the API feeder is calculated and this flow rate when deducted from the total flow rate gives the set point for the excipient feeder flow rate. Thus, actuating the API ratio actuates the flow rates of the two feeders. A comparison between the two actuators for a feedback controller has been discussed in the "Results and Discussions" Section. Actuating the API ratio changes the API ratio and thus $C_{\text{granulator, inlet}}$ varies linearly with respect to the actuator. However, actuating only the flow rate set point of the excipient feeder, changes the flow rate of the excipient feeder only which makes $C_{\text{granulator, inlet}}$ vary nonlinearly with respect to the actuator. Figure 6 describes the relationship between the actuator candidate and the composition of API in granules theoretically. The primary vertical axis on the left represents the API Ratio and the secondary vertical axis on the right represents the flow rate of the excipient feeder. It can be seen from the figure that the relationship between API Ratio and API composition in granules is linear, whereas the relation between flow rate of excipient feeder and API composition in granules is non-linear.

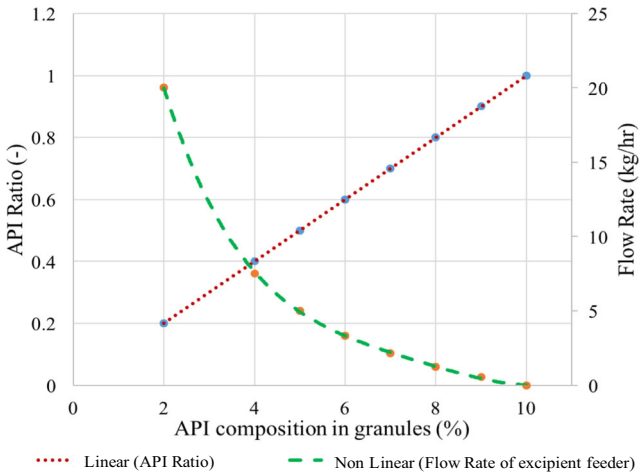

Fig. 6 Actuator vs API composition in granules for the two actuator candidates

$$C_{\text{granulator,inlet}} = \frac{C_{\text{API feeder}} F_{\text{API feeder}}}{F_{\text{API feeder}} + F_{\text{Excipient feeder}}} \tag{6}$$

$$\text{API ratio} = \frac{C_{\text{granulator,inlet}}}{C_{\text{API feeder}}} = \frac{F_{API\ feeder,SP}}{F_{\text{API feeder,SP}} + F_{\text{Excipient feeder,SP}}} \tag{7}$$

Control Relevant Transfer Function Model

The model for the feedforward controller can be given as a ratio of the disturbance transfer function to the process transfer function $(-G_d/G_p)$ which is found by equating the characteristic equation to zero [21]. In order to develop this transfer function model for the feedforward controller, a transfer function model for disturbance was developed which would relate the disturbance to the control variable. Next, process models for the two feeders and the granulator were developed. These models were developed in the System Identification Toolbox of MATLAB using step change data. The input and output data used for each process are as described in Table 2. The transfer function models as given in Table 2 are developed based on inputs/outputs responses. Note that, the transfer function models depend on various factors including process, formulation and operating conditions and therefore, need to be re-estimated if there will be any any chnages in the manufacturing scenario. The transfer function models given in Table 2 are for demonstrattion purposes.

The feeder transfer functions (G_{p1} and G_{p2}) relate the feeder screw rotational speed to the outlet flow rate through a second-order transfer function with no zero and two poles. The pole-zero map and the bode diagram are as shown in Fig. 7. The map shows that the two poles are imaginary and the feeder process is stable but oscillatory. The bode diagram gives information about the gain margin and the phase margin. Typical design specification requires that the gain margin be greater than 1.7 dB and the phase margin be greater than 30°. For the feeder transfer function, both the phase margin and the gain margin are infinity. The process dead time was relatively smaller and therefore, has been ignored. The granulator transfer function (G_{p3}) relates the inlet API composition to the outlet API composition through a first order transfer function with one zero and one pole. The pole-zero map and the bode plots for it are shown in Fig. 8 and it can be seen that the system is stable and non-oscillatory. The gain margin and phase margin for this system are both infinity. Similarly, the disturbance transfer function model relates the API composition at feeder 1 outlet to the API composition at the outlet of the granulator. The model is based on a step change in

Table 2 Process transfer function model

Transfer functions	Inputs	Outputs	Models
1. $G_{p1}(s)$	Screw rotational speed	API + excipient flow rate	$\frac{0.0247}{25s^2+0.5s+1}$
2. $G_{p2}(s)$	Screw rotational speed	Excipient flow rate	$\frac{0.0247}{25s^2+0.5s+1}$
3. $G_{p3}(s)$	API composition	API composition	$\frac{0.7379s+0.03702}{s+0.03613}e^{-20s}$
4. $G_d(s)$	API composition at feeder 1 outlet	API composition at granulator outlet	$\frac{1}{s^2+0.4204s+0.1501}e^{-25s}$

concentration. The transfer function model is a second-order transfer function model with two imaginary poles. The pole-zero map is shown in Fig. 9 where it can be observed that the system is stable but oscillatory. The gain margin for the disturbance transfer function is infinity while the phase margin is 17.5464°.

Design of Control System

As discussed earlier, a combined feedforward/feedback control loop helps to achieve the desired controlled response. In this section, the feedforward controller model was developed for a continuous twin screw granulation process. The control variable for the respective control strategy is the concentration of API at the outlet of the granulator C_{out}. A pre-blend of API and excipient is the feed through one feeder and pure excipient is the feed through the second feeder. Feeders and a twin screw granulator are the two unit operations around which the control loops have been built. This feedforward controller model is specific to a particular formulation since it depends on the concentration of API in the pre-blend. Control loops with NIR sensing have been added to the open loop process flowsheet shown in Fig. 1 which gives the closed loop process flowsheet shown in Fig. 10. An NIR sensor is mounted at the exit of feeder 1, which measures the concentration of API exiting feeder 1 and sends the measured value to the feedforward controller. The RTD model described in the "Continuous Granulation (TSG)" Section predicts the concentration of API at the exit of the granulator and this predicted value of concentration is sent to the feedback PID controller. Together, the feedback controller and the feedforward controller manipulate the flow rate of the excipient feeder (feeder 2). The excipient feeder flow rate is then controlled by manipulating the screw rotational speed. The combined feedforward/feedback control for continuous tablet manufacturing process via wet granulation has been designed in accordance with that described in Singh et al. [9].

Combined Feedforward/Feedback Control System Architecture

The architecture of control option 1 (see Table 1: Nonlinear actuation) is shown in Figure 11 and consists of four control loops. Loops 1 and 2 are the built-in feedback control loops for the two feeders. Loop 3 is the master feedback controller and loop 4 is the feedforward controller. The controlled variables, inputs, and outputs for the controller structure have been listed in Table 3.

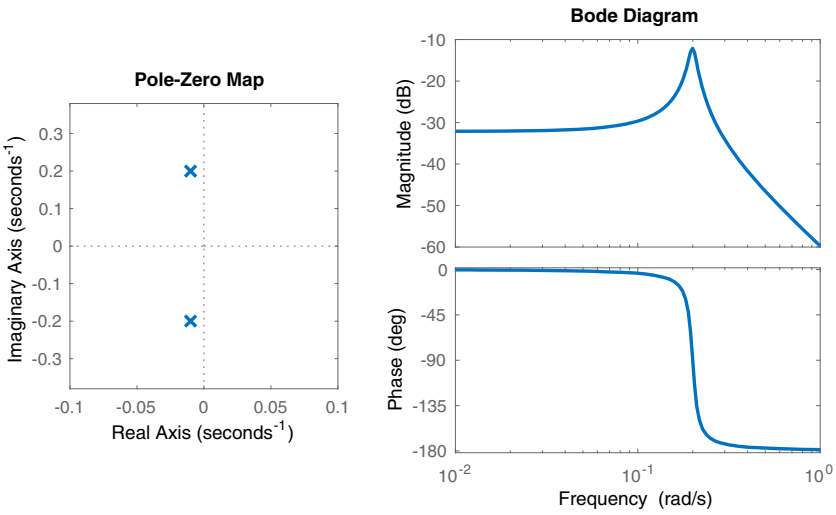

Fig. 7 Pole-zero map and bode plot for feeder transfer function

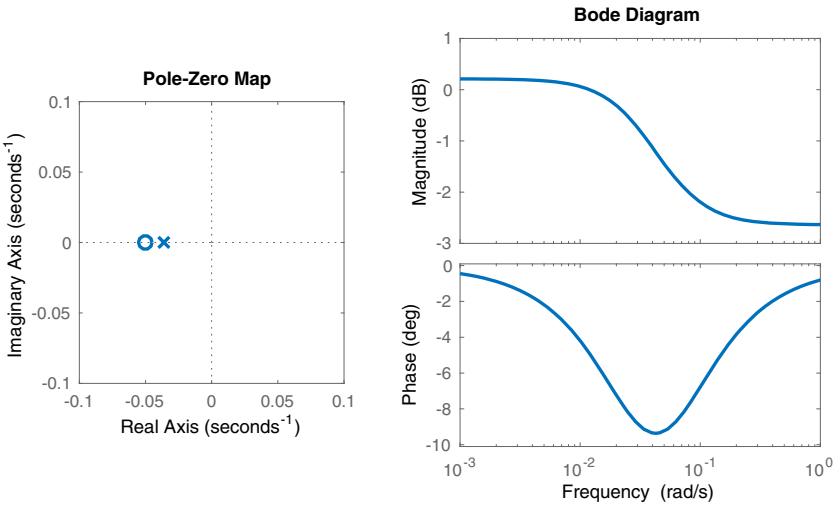

Fig. 8 Pole-zero map and bode plot for granulator transfer function

Control loop 1 is the built-in feedback loop for feeder 1 (feeder API - excipient blend) and works on the loss-in-weight feeder concept. The feedback loop is the classical PID-based controller. The built-in PID controller model in gPROMS was used. This loop controls the output flow rate of 'API and excipient blend' from feeder 1 by manipulating the screw rotational speed of the feeder through the PID controller. As given in Table 3, the deviation of the flow rate from the set point that would be predetermined is the input to the PID controller and the screw rotational speed is the output.

Control loop 2 is also the built-in feedback loop for feeder 2 (excipient-only feeder) and works on the same concept as control loop 1. This loop controls the output flow rate of excipient from feeder 2 by manipulating the screw rotational speed of the feeder. The input to the PID is the deviation of flow rate from set point that is given by the outputs of the master feedback controller and the feedforward controller.

Control loop 3 is the master feedback controller which is also the classical PID-based controller. The concentration of API at the exit of the granulator is about 4% as seen in Fig. 10. For this study, we proposed to build an RTD model for the twin screw granulator as described in the "Continuous Granulation (TSG)" Section that would predict the outlet concentration of API from the granulator and which would be an input to the feedback controller. The input to the PID is the API concentration from the granulator and the output is the set point it provides to control loop 2 (feeder 2 flow rate set point) along with the feedforward controller.

Loop 4 is a feedforward control loop. The real-time measurement of the API concentration at feeder 1 outlet is the input of this controller. The real-time measurement of concentration can be done by the NIR sensor mounted at the exit of the feeder. Since the concentration of API coming out of feeder 1 is about 12%, its measurement via NIR is possible. The model for the feedforward controller is developed using transfer function

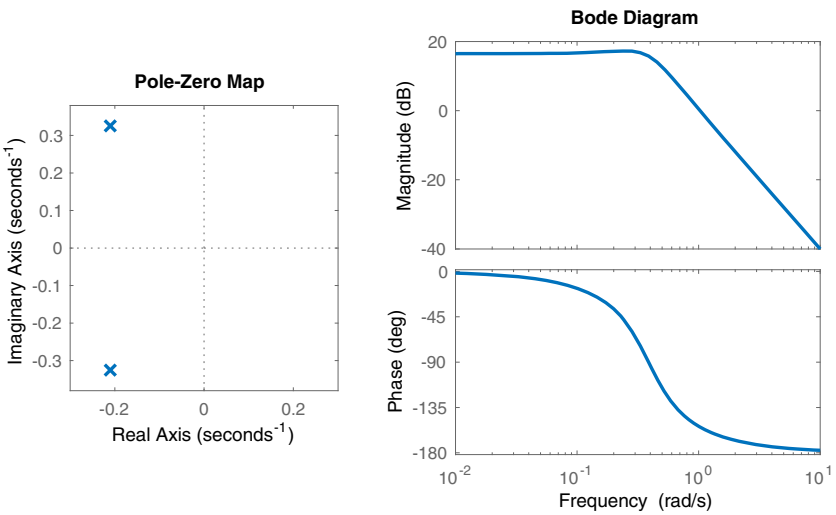

Fig. 9 Pole-zero map and bode plot for disturbance transfer function

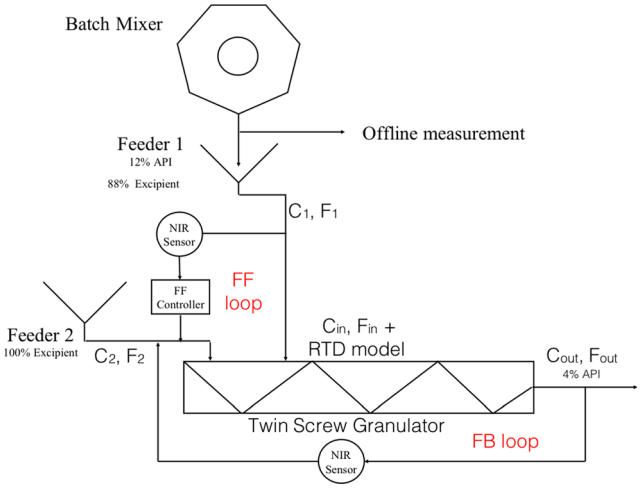

Fig. 10 Integrated continuous wet granulation process flowsheet with control loops. FF, feedforward; FB, feedback

model in MATLAB. The output of this controller is the set point of control loop 2 along with the master feedback controller. Note that, the feeder 2 flow rate set point is the summation of outputs of both feedforward and feedback controllers.

Architecture of the combined feedforward/feedback control system in case of linear actuation (control option 2, see Table 1) is similar to that shown in Fig. 11 and listed in Table 3; the only difference is that the output of the feedback and feedforward controller provides the "API ratio set point" instead of "excipient flow rate set point." The feeder 1 and feeder 2 set points are then calculated based on the API ratio set point. The supervisory control loops can be based on PID or MPC algorithms.

PID Controller Parameters Tuning

It can be noted from Table 3 that three PID controllers have been used. Tuning the controller is essential to achieve the desired performance. There are several methods and rules to achieve controller tuning, and it could be either a heuristic method or it could be defined as an optimization problem [22]. The PID controller has three tuning parameters, proportional (P), integral constant (I), and derivative constant (D). Simulink provides an inbuilt methodology for the tuning of these three parameters. This methodology follows an optimization problem where the objectives include closed loop stability, adequate performance, and adequate robustness. For a single-input/single-output system, the PID tuner achieves the above objectives by balancing between the controller performance and robustness. The PID tuner considers all the blocks in the control loop except itself and computes a linear model of the plant. Based on the open loop frequency response of this linear model, it computes an initial set of parameters. Changing the response time, bandwidth, transient behavior, or phase margin in time domain or frequency domain computes a new set of PID parameters. This automatic tuning selects a design that balances between set point tracking and disturbance rejection. Preference can be given to either of the performance measures on the PID Tuner interface. The PID parameters for the three feedback control loops are given in Table 4. Plugging the three parameters in Eq. 8 gives the controller transfer function. Note that there are different ways of representing a PID controller and its tuning parameters. In

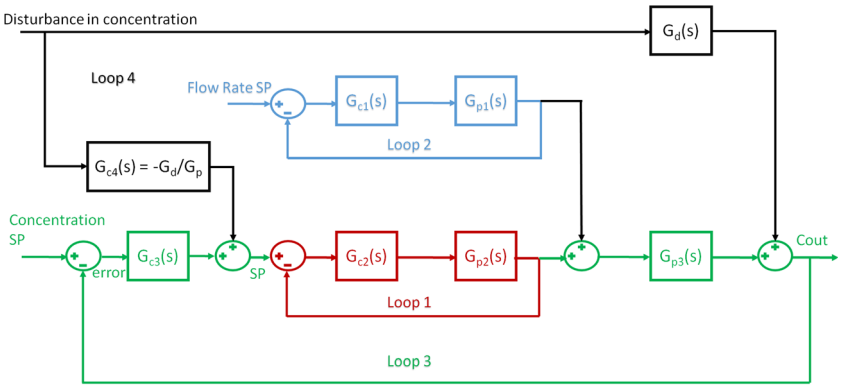

Fig. 11 Architecture of the combined feedforward/feedback control system in case of nonlinear actuation (control option 1)

Table 3 Controller configuration in case of nonlinear actuation (control option 1)

Controller loops	Controller	Controlled variables	Inputs	Outputs
1. Feedback	$G_{c1}(s)$	API + excipient flow rate	Deviation of API + excipient flow rate from set point	Screw rotational speed
2. Feedback	$G_{c2}(s)$	Excipient flow rate	Deviation of excipient flow rate from set point	Screw rotational speed
3. Feedback	$G_{c3}(s)$	API concentration	Deviation of API concentration from set point	Excipient flow rate set point
4. Feedforward	$G_{c4}(s)$	–	API concentration	Excipient flow rate set point

Table 4 PID controller tuning parameters

Controllers	Proportional gain (P)	Integral constant (I)	Derivative constant (D)	Filter coefficient (N)
G_{c1}	200.270	80.110	1800.170	104.650
G_{c2}	200.270	80.110	1800.170	104.650
G_{c3}	18.033	0.891	− 160.572	0.084

this manuscript, the PID and its tuning parameter forms as available in Simulink (Mathworks) have been used for Simulink-based simulation. The PID controller tuning parameters depend on various factors including process, formulation, and operational conditions. Therefore, any changes in plant will need retuning of the controllers. It is a good practice to retune the controllers regularly.

$$G_c(s) = P + I\frac{1}{s} + D\frac{N}{1 + N\frac{1}{s}} \tag{8}$$

In the combined feedforward/feedback control system, either the feedback controller or the feedforward controller can be tuned first. The feedback control system can be tuned once the process transfer function G_p is identified which in our case is given by Eq. 9. Once, the feedback controller is tuned, the disturbance transfer function model can be identified through experiments as given in Table 2. Thus, the feedforward controller model is developed as discussed in the "Control Relevant Transfer Function Model" Section. We have assumed our plant and disturbance model to be accurate and hence the feedforward controller tuning has not been considered. However, the feedforward controller can be tested by simulating only feedforward control loop. If there is an offset in the response variable, it indicates an error in the feedforward gain K_{ff}. The dynamic tuning parameters, i.e., the lead and lag time is determined by removing feedback control action and using tuning parameters for feedforward control described in the literature [22]. It should also be noted that the feedforward controller model changes with any change in the process or the material and hence is specific to a given process and formulation.

$$G_p = \left(G_{p1} + G_{p2}\right) \times G_{p3} \tag{9}$$

Development of Model Predictive Control

After the development of a PID-based control system architecture, a feedback-based model predictive controller was developed. The feedback-based PID controller was replaced with a single MPC that had one input and one output. Thus, a single-input-single-output MPC was developed. The input was API composition in granules and the output was API ratio. Noise in the measured data was incorporated into the model as measured disturbance. The MPC was designed using a MPC block which designs the controller by using a linearized plant model. Thus, a linear time invariant (LTI) model is first developed for the process and this model is then imported into the MPC toolbox. A default MPC model is then developed through optimization of an objective function at each control interval. Thus, MPC employs a receding control horizon scheme. The sampling time was set at 2 s, the prediction horizon was set at 38 s, and the control horizon was set as 2 s. The built-in MPC tuning was used to tune the three tuning parameters and follows the Integral of Time Absolute Error (ITAE) criteria. The three tuning parameters are input weights, output weights, and rate weights. The output weight of a variable determines the amount of control action taken for that variable. If the output weight for a variable is large, the controller tries to minimize the error for that variable. Similarly,

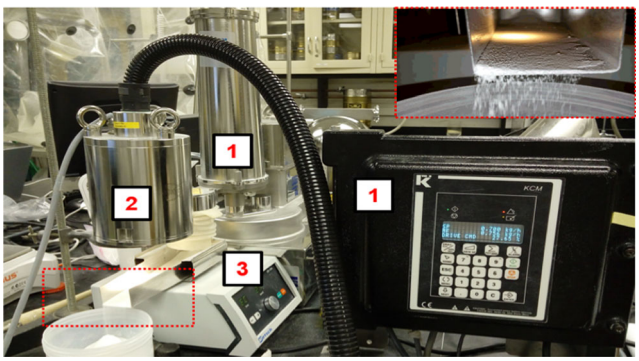

Fig. 12 Experimental setup. (1) K-Tron MT12 feeder. (2) Bruker Matrix FT-NIR. (3) Vibratory feeder

Table 5 Calibration blends (in % *w/w*) needed to construct the "calibration model 1"

APAP (% *w/w*)	SMCC (% *w/w*)	MgSt (% *w/w*)
10.50	88.50	1.00
12.75	86.25	1.00
15.00	84.00	1.00
17.25	81.75	1.00
19.50	79.50	1.00

APAP acetaminophen, *SMCC* silicified microcrystalline cellulose, *Mg St* magnesium stearate

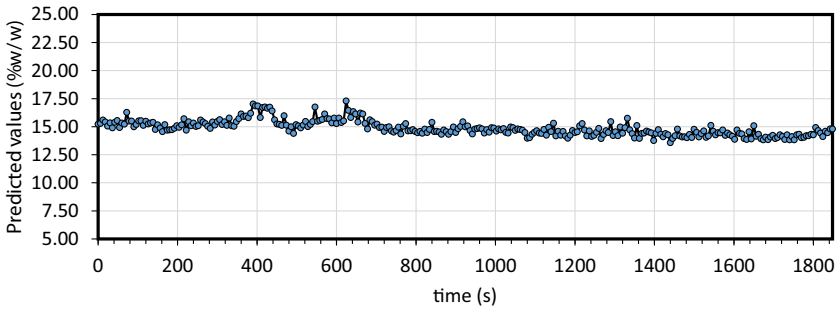

Fig. 13 Predicted values from a test run at the proposed experimental setup

Table 6 Evaluation of an independent run to test the calibration model and the experimental setup

2-PLS factors MSC, 9500–7500 cm^{-1}					
RMSEP	RSEP (%)	Average	RSD (%)	Stdev	Bias
0.68	4.53	14.86	4.50	0.67	− 0.14

the input weight helps in keeping the actuator variable at the nominal value while the rate weight determines the number of control steps to be taken.

Real-Time Monitoring for Combined Feedforward/Feedback Control

Real-time monitoring of different variables for pharmaceutical tablet manufacturing has been an area of research for many years. The most versatile tool among the various techniques is NIR. Real-time monitoring of powder bulk density has been previously reported by Román-Ospino et al. [23]. Vanarase et al. have demonstrated the use of NIR spectroscopy for monitoring drug concentration in a continuous powder mixing process [13]. In this study, the use of NIR spectroscopy for real-time measurement of API composition at the outlet of the feeder as well as the outlet of the twin screw granulator has been demonstrated. The objective of this section is to create an experimental setup that can accomplish proper sampling strategies which can be used to implement and validate the proposed combined feedforward/feedback control strategy.

NIR spectroscopy has been used for measurement of drug concentration of the powder blend at the outlet of feeder 1. This real-time measured drug concentration signal is used as an input to the feedforward controller. The NIR has also been used for real-time monitoring of drug concentration in granules at the outlet of the granulator which is provided as an input to the feedback controller. The same NIR can also be used to monitor moisture content of the granules but an additional calibration model is needed to accomplish this. Therefore, in total, two NIR sensors and three calibration models are needed. The same experimental setup has been used to generate open loop process data needed to build the model and feedforward controller.

Development of an Experimental Setup for Building NIR Calibration Model

An experimental setup was constructed for one-dimension (1-D) sampling at the feeder outlet as shown in Fig. 12. A proof of concept was performed where a loss-in-weight feeder was used to transfer pre-blend into a vibratory feeder. The vibratory feeder acts as a conveyor providing the surface in 1-D approach for the near infrared (NIR) spectral acquisition. Also, the built-in stainless steel does not interfere with measurement.

The near infrared instrument was a MATRIX-F FT-NIR process spectrometer from Bruker Optics (Billerica, MA, USA) controlled with the OPUS 6.5 software. The “control process” feature was used to acquire spectra in continuous mode. The resolution used was 16 cm^{-1}, 32 scans for background and sample. Figure 12 shows the emission head from the NIR instrument containing the source. The reflected light is transferred to the interferometer via fiber optic.

Table 7 Experimental design used for batch granules

Number	Water (% *w/w*)	APAP (% *w/w*)	MCC (% *w/w*)	Total (% *w/w*)
1	4.00	2.50	93.50	100.00
2	4.00	4.50	91.50	100.00
3	6.00	3.50	90.50	100.00
4	6.00	3.50	90.50	100.00
5	8.00	2.50	89.50	100.00
6	8.00	4.50	87.50	100.00

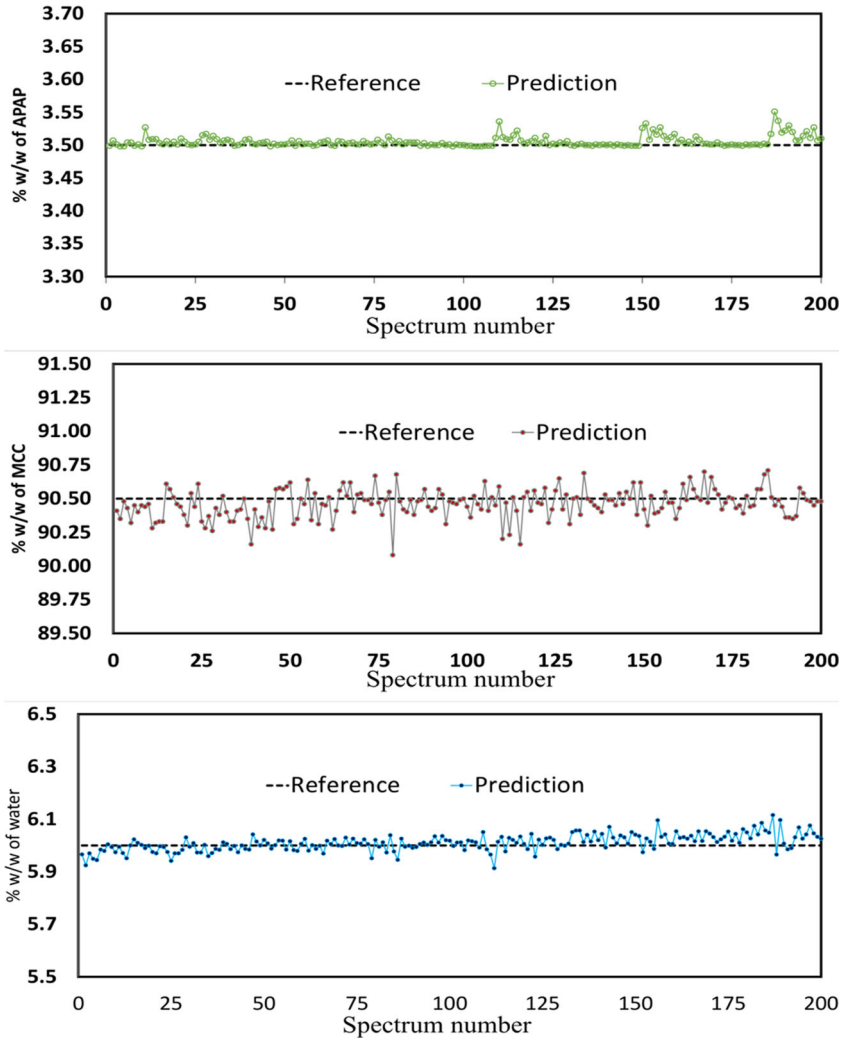

Fig. 14 Predicted values for API (APAP), excipient (MCC), and water concentration in granules, 204 spectra acquired in approximately 23 min

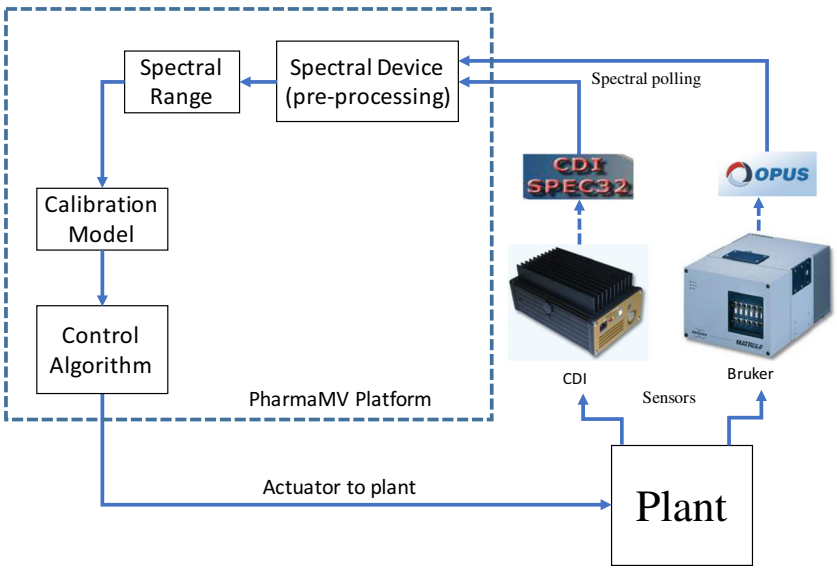

Fig. 15 Integration of control hardware and software

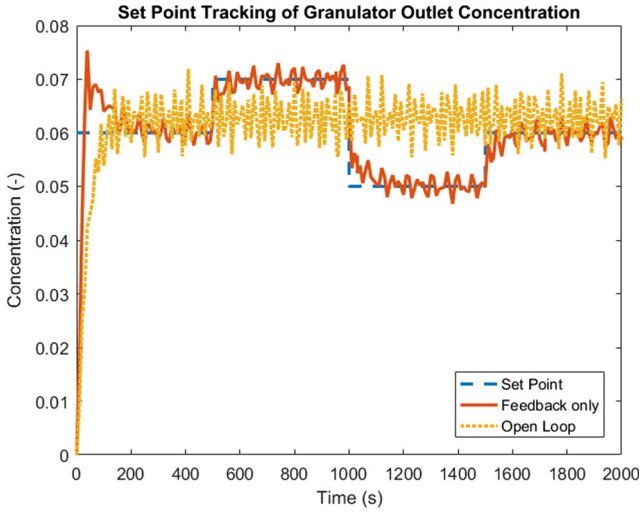

Fig. 16 Comparison of open loop and closed loop response (set point tracking)

Real-Time Monitoring of API Concentration at Feeder Outlet

The real-time monitoring of API concentration at feeder 1 outlet (consisting of blend of API and excipient) is needed to enable the feedforward controller. The experimental setup as shown in Fig. 12 was used for constructing an NIR calibration model for drug concentration measurement. Blends of different API concentration were prepared in a V-blender and transferred to the feeder. The blend composition used to build the NIR calibration model is given in Table 5. Online NIR calibration approach was used. The blend was fed from the MT-12 feeder with a fixed flow rate set point of 0.700 kg/h to the vibratory feeder. One additional blend (15% APAP, 84% SMCC, 1% MgSt) was prepared for testing the model. More than 300 spectra were acquired for each blend.

Different calibration models were constructed and evaluated based on the lowest root mean square error of prediction (RMSEP) value to identify the best projection to latent structures (PLS) model. An independent 15 %w/w blend was used for this test. The best results were obtained using the spectral range 9500–7500 cm^{-1}, multiplicative scattering correction (MSC) as data pretreatment, and two latent variables. The performance of NIR calibration model for real-time monitoring of API composition at feeder outlet is shown in Fig. 13. The test run (with API composition of 15%) was performed to evaluate the predictive capability of the NIR calibration model. As shown in Fig. 13, the API composition was successfully monitored at the feeder outlet.

The results of evaluation of a test blend that challenges the calibration model and the proposed experimental setup is given in Table 6. The relative standard error of prediction (RSEP) (%) values obtained were considered appropriate for this proof of concept experiment.

Real-Time Monitoring of Granules at Granulator Outlet

The API composition and moisture content of the granules are required to be monitored at granulator outlet. The API composition is needed for proposed feedback control strategy. The

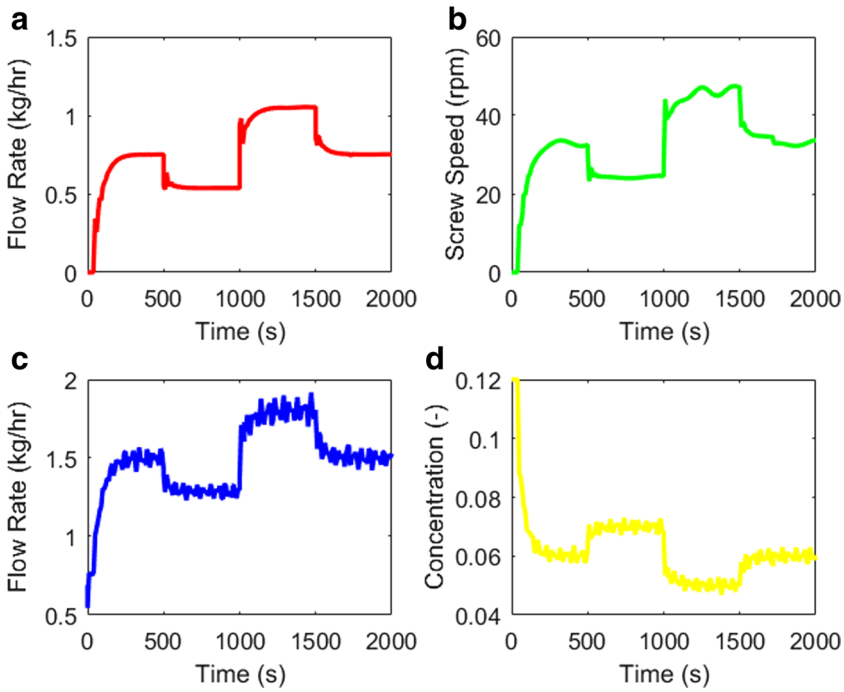

Fig. 17 **a** Manipulated variable, i.e., set point for excipient feeder flow rate. **b** Screw speed of excipient feeder. **c** Total inlet flow rate to Granulator. **d** Total inlet concentration to granulator

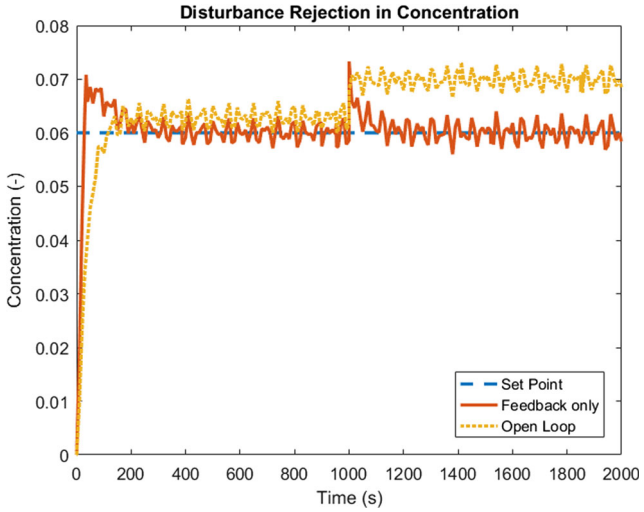

Fig. 18 Comparison of open loop and closed loop (disturbance rejection–step disturbance in concentration)

samples to develop the NIR calibration model were produced using batch granulation process. A full factorial design of experiment was performed for batch granules for three levels of water content, MCC, and acetaminophen. A batch granulator was used under constant impeller and chopper speed for all calibration granules and 400 g batches were prepared for each concentration level. The experimental design used to build the NIR calibration model for API composition and moisture content is given in Table 7.

Samples were stored at room temperature in double sealed bags for 24 h before spectral acquisition. NIR spectral acquisition was performed by using the same 1-D experimental setup as mentioned in the "Real-Time Monitoring of API Concentration at Feeder Outlet" Section. Calibration models were constructed for each component in the formulation. Figure 14 shows the PLS prediction of API, MCC, and water for a test batch of granules. The total number of spectra was 204 and the acquisition time was 7 s/spectrum. The gravimetric reference value of APAP, MCC, and water was 3.50, 90.50, and 6.00% *w/w* respectively. The feeder flow rate set point was kept at 0.700 kg/h. The prediction model of MCC is not needed to enable the proposed control system since the control action is based on API concentration measurement.

Integration of Control Hardware and Software for Implementation

In order to implement the control system, control hardware and software are integrated with the plant. First, the process consisting of two feeders and a granulator are integrated under the Thermo Fisher programmable logic controller (PLC) platform. The PLC communicates the process data to a remote computer for data analysis. The remote computer is equipped with PharmaMV control platform (Perceptive Engineering) that reads the process data from the PLC via OPC (OLE for process control). This established connection reads process variables and communicates actuator signals back to the plant as input. NIR sensors are integrated with the control platform and plant for real-time monitoring of API composition. The sensor operating software collects the spectra and sends the information to the PharmaMV Real Time System via spectral file polling. The Real Time System consists of the spectral device, spectral range, and the calibration model previously

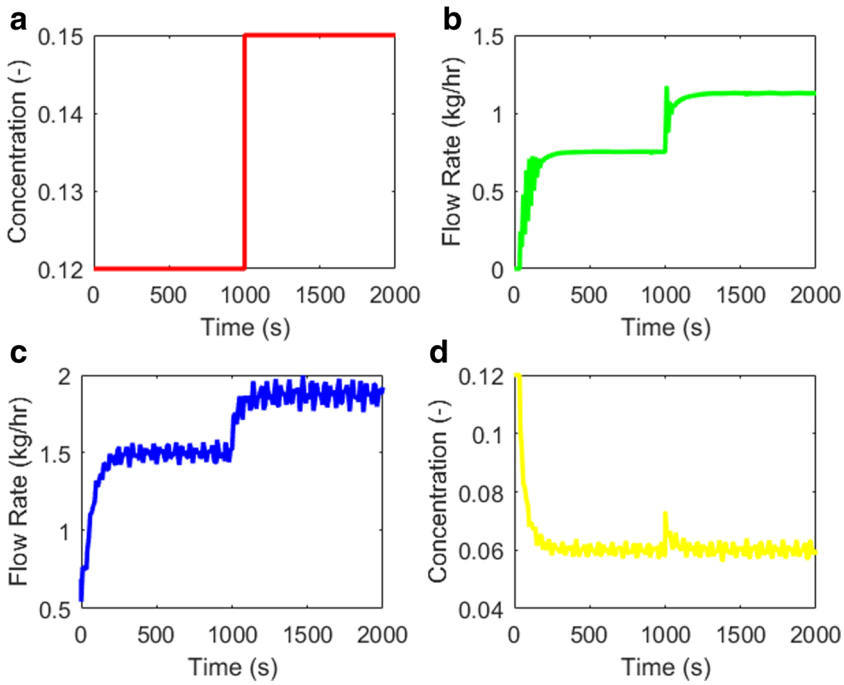

Fig. 19 **a** Step disturbance in concentration. **b** Manipulated variable, i.e., set point for excipient feeder flow rate. **c** Total inlet flow rate to granulator. **d** Total inlet concentration to granulator

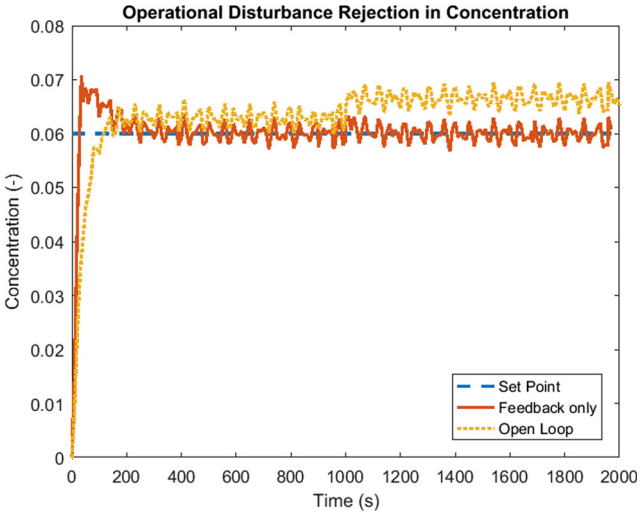

Fig. 20 Comparison of open loop and closed loop (disturbance rejection–step disturbance in API flow rate)

developed in the "PharmaMV Development System" which is used for the real-time prediction of API composition. After the integration of process data and PAT sensors, the control loops are added for advanced process control. The controller connects the actuator variables with the controlled variables.

The control hardware and software integration is shown in Fig. 15. As seen in the figure, the API composition in granules and at the feeder outlet are measured by NIR spectrometers. The spectrometers are operated by their individual software which collects the spectra in an SPC file and transfers these files to the PharmaMV platform via spectral polling. The PharmaMV platform uses a calibration model previously built in the development mode to give real-time predictions. These real-time predictions of API composition are used as an input to the controller and an output is calculated based on the control algorithm in place. The output is the API ratio which goes through a calculation block that calculates the respective flow rates of the two feeders by maintaining the production rate constant.

Results and Discussions

Modeling and simulation is gaining increasing importance in pharmaceutical industry. The use of process models in pharmaceutical manufacturing will help reduce cost and enhance quality of products [24]. This section focusses on evaluating the performance of the combined feedforward/feedback control through process simulation before implementing it on the pilot plant. The primary focus is on set point tracking and disturbance rejection. For set point tracking, a step change in concentration was introduced and the ability of the controller to track the change was observed. For disturbance rejection, random noise was passed through the system and the ability of the controller to reject the disturbance was evaluated. The quality of the controlled response has been discussed with the help of various performance evaluation parameters.

Evaluation of Closed Loop Control for control option 1

Set Point Tracking

As discussed in the "Integration of the Unit Operations Model" Section, the unit operation models were developed and simulated in gPROMS and the open loop response of

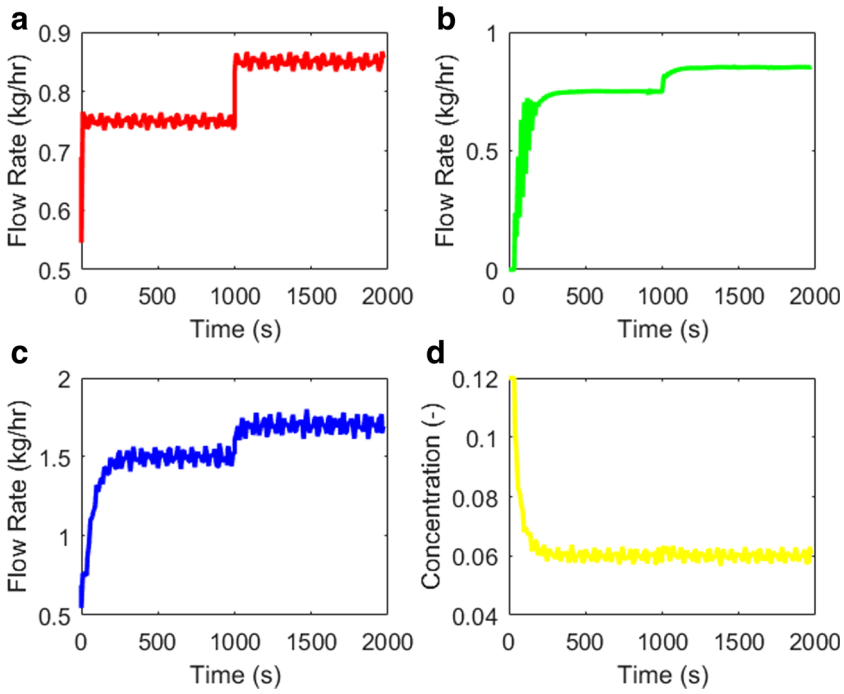

Fig. 21 **a** Step disturbance in API flow rate. **b** Manipulated variable, i.e., set point for excipient feeder flow rate. **c** Total inlet flow rate to granulator. **d** Total inlet concentration to granulator

the integrated flowsheet model was analyzed. Variables important for the control of API concentration at the exit of the granulator were systematically studied. In order to highlight the importance of automatic control system for continuous wet granulation process, the open loop response was first compared with feedback-only closed loop response. As shown in Fig. 16, the feedback-only control tracked the predefined set point which is not possible in open loop operation. Set point tracking is essential for our process to provide for bump-less transfer from one set point to another set point. This also makes the process robust to a range of concentrations.

In Fig. 17, we have described four important variables that are affected or manipulated by changing the set point in the feedback control loop. Figure 17a shows the response of manipulated variable (the set point for the excipient feeder flow rate) as a function of time. The feedback controller provides the necessary set point to the PID controller of the excipient feeder. As can be seen, the manipulated variable also follows the set point. When the concentration is increased, the set point for the excipient feeder is lowered indicating that the excipient must flow at a lower flow rate thus increasing the concentration. Figure 17b shows the response of screw speed of the excipient feeder (in revolutions per minute) as a function of time and it behaves similarly to the excipient feeder flow rate set point. Figure 17c shows the response of total inlet flow rate to the granulator. As the excipient flow rate is decreased at 500 s to account for the increase in concentration, the total inlet flow rate also decreases because the flow rate from the API feeder is held constant. Figure 17d shows the total inlet concentration of API entering the granulator as a function of time. As the excipient flow rate is reduced, the concentration of API entering the feeder also increases according to Eq. 6.

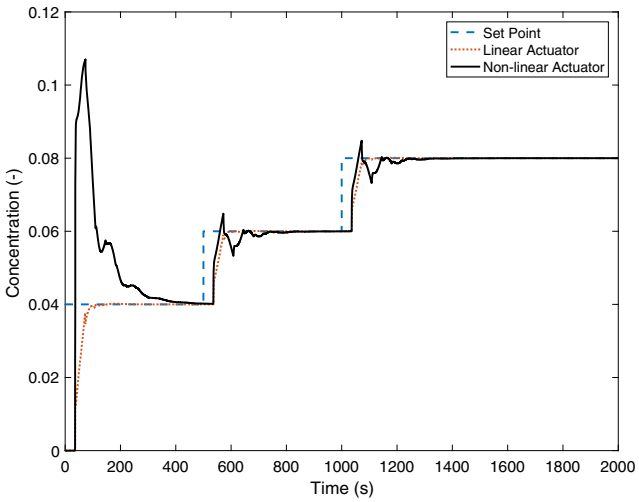

Fig. 22 Comparison of the feedback control response for API composition in granules for the two actuator candidates

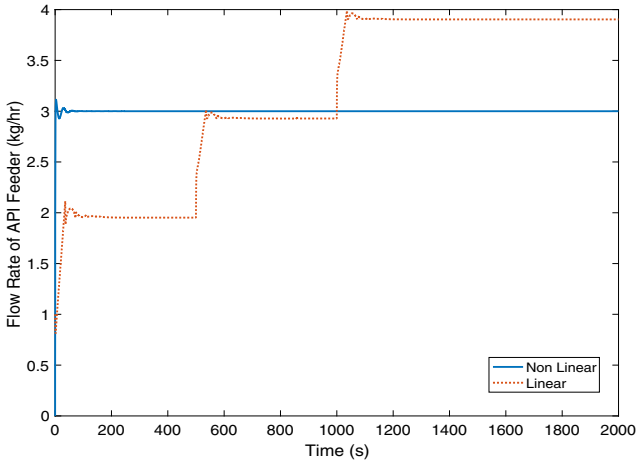

Fig. 23 Flow rate of API feeder for the two actuators

Disturbance Rejection

One of the primary reasons to use the control system is to reject the effect of known and unknown disturbances on CPP's and CQA's in real time. Therefore, the disturbance rejection ability of the control system has been evaluated in this section. In the considered process, there can be a disturbance in the concentration exiting the feeder due to non-uniformity in the pre-blend fed to the API feeder. There could also be disturbance in the flow rate of the API feeder and that could affect the concentration of the granules exiting the granulator. The controller's ability to reject the effect of these two types of disturbances is discussed in the following sections.

Step Disturbance Rejection (Concentration)

The first disturbance rejection considered is a step change in concentration. The set point for the granulator outlet concentration was maintained at 6%. A disturbance was then introduced at 1000 s where the concentration from the outlet of the

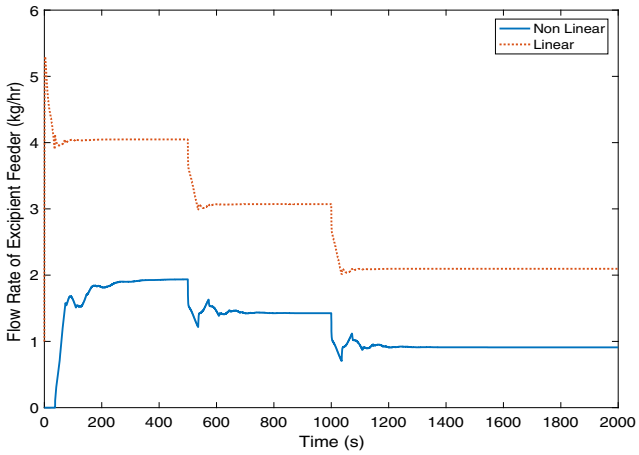

Fig. 24 Flow rate of excipient feeder for the two actuators

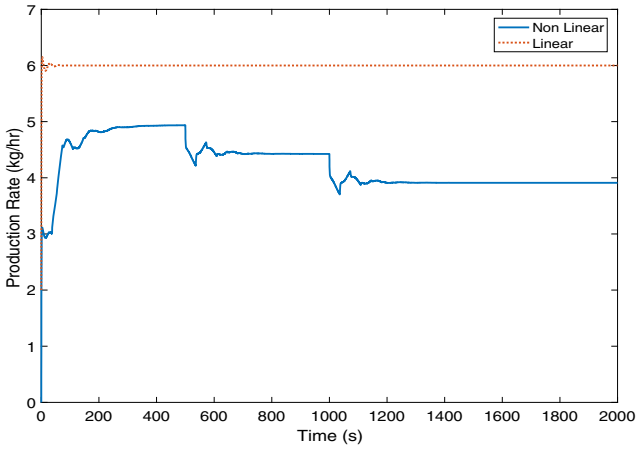

Fig. 25 Total production rate for the two actuators

API feeder was changed from 12 to 15%. In Fig. 18, the open loop response shows an increase in the granulator outlet concentration after 1000 s. This is in accordance with how the process would operate in the absence of control. However, the feedback control loop has a sudden increase of concentration at 1000 s and then settles very quickly back to the set point of 6%. Thus, it is shown that feedback control rejects this disturbance effectively.

Figure 19a shows the step disturbance from 12 to 15% introduced in API concentration at 1000 s within the API Feeder. As can be seen in Fig. 19b, the manipulated variable (set point for the excipient feeder flow rate) increases due to an increase in the inlet API concentration and thus helps in maintaining the outlet API concentration constant at 6%. As mentioned in the "Set Point Tracking" Section, Fig. 19c and d varies according to Eq. 6.

Operational Disturbance Rejection (API Feeder Flow Rate)

The second disturbance rejection considered is an operational disturbance. It is a step disturbance in the flow rate of the API feeder. This disturbance accounts for any changes made in the throughput of the process. In this analysis, the disturbance was introduced at 1000 s by changing the flow rate from 0.75 to 0.85 kg/h. Figure 20 shows the effect of this disturbance on the outlet concentration for open loop and feedback-only loop as a function of time. The open loop responds to the increase in the API flow rate by increasing the outlet concentration after 1000 s. This follows Eq. 8, since the granulator inlet API concentration increases when the API flow rate increases. However, the feedback control loop maintains the concentration at the set point after the disturbance has been introduced.

Figure 21a shows a step disturbance in the API feeder flow rate as a function of time. The variable manipulated by the feedback controller to maintain the concentration is the set point of the excipient feeder given by Fig. 21b. As the API feeder flow rate increases after 1000 s, the excipient feeder flow rate also increases to maintain the inlet concentration to the granulator given in Fig. 21d and thereby controlling the outlet concentration. Thus, the total feed flow rate entering the granulator increases and this is depicted by Fig. 21c.

The above two analyses confirm that feedback controller rejects most of the disturbances; however, as seen in the two figures, there are some random disturbances propagated through the granulator. Therefore, a feedback controller alone is not sufficient to reject these disturbances. Thus, it was proposed that a combined feedforward/feedback controller be implemented for this particular process. In the "Comparison of Linear and Nonlinear Acuators" Section, we discuss and

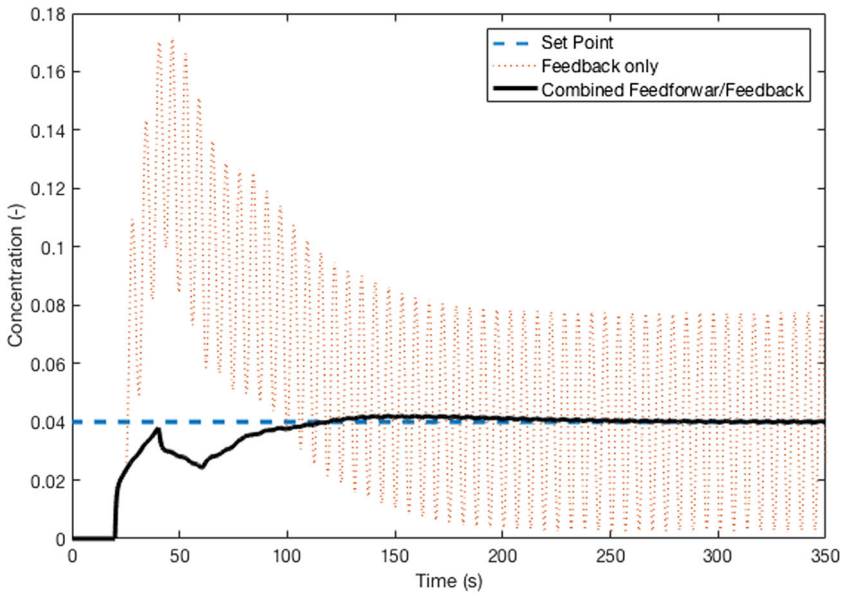

Fig. 26 Comparison of combined feedforward/feedback control with feedback-only control (random disturbance)

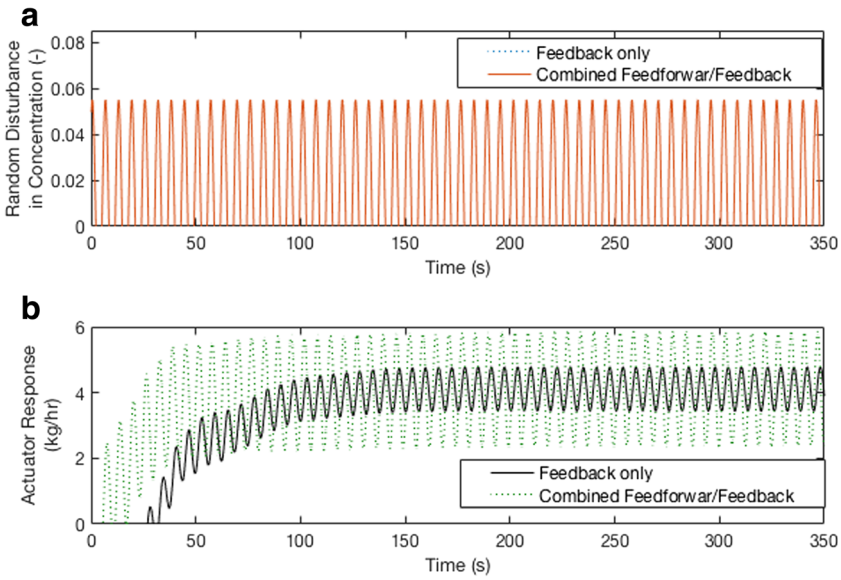

Fig. 27 **a** Disturbance (random) in concentration. **b** Actuator response, i.e., set point of excipient feeder flow rate (kg/h)

evaluate the performance of the combined feedforward/feedback control strategy.

Comparison of Linear and Nonlinear Actuators

In order to evaluate combined feedforward/feedback control strategy and MPC control strategy, simulation was performed using Simulink (Mathworks) because the gPROMS simulation platform currently does not have the capability to add feedforward controllers or MPC controller. Thus, the gPROMS flowsheet model was transferred into Simulink. The relevant transfer function models for the various unit operations have been described in the "Control Relevant Transfer Function Model" Section. These transfer function models were fit to the data generated by the gPROMS model so that the two integrated flowsheet models were similar. Open loop analysis was also carried out on the integrated Simulink model to ensure that the model responded accurately. Before discussing the two control options, a comparison was conducted between the two actuators.

Figure 22 compares the response of a basic feedback (PID) control when a linear actuator (API ratio) is used versus when a nonlinear actuator (flow rate set point of excipient feeder) is used. As can be seen from the figure, when the linear actuator is used, the control response is similar to that of a first order response with no overshoot. However, when a nonlinear actuator is used, the response is similar to that of a second-order response with some overshoot. The rise time for the linear actuator is 95 s which is slightly higher than the rise time for the nonlinear actuator which is 60 s. However, the settling time for the linear actuator is 140 s while the settling time for the nonlinear actuator is 336 s.

Figure 23 shows the response of API feeder flow rate for the two control options. It can be seen that the flow rate of API feeder remains constant for the nonlinear actuator; however, the flow rate of API feeder changes with each step change for the linear actuator. Thus, in the case of nonlinear actuator, the input disturbance in API concentration would be minimal in comparison since the flow rate of the API feeder remains constant.

Figure 24 describes the flow rate of excipient feeder for the two control options. In this case, for both control options, the flow rate changes based on the step change. However, for linear actuator, the production rate as shown in Fig. 25 remains constant whereas the production rate for nonlinear actuator varies. Thus, in case of linear actuator, the composition of API as well as the production rate are controlled while in case of nonlinear actuator only, the composition of API is controlled. The production rate for the two cases is different before 500 s because as can be seen in case of nonlinear actuator, the API composition in granules is quite high and it takes a long time for the response to settle. Thus, the controller

Table 8 Performance evaluation of combined feedforward/feedback control vs. feedback-only control (random disturbance in concentration)

Controller	RMSE (−)	ITAE (−) s^2	ISE (−)^2 s	IAE (−) s
Combined feedforward/feedback	0.006	1410.157	0.257	14.417
Feedback-only	0.032	120,816.070	10.184	265.834

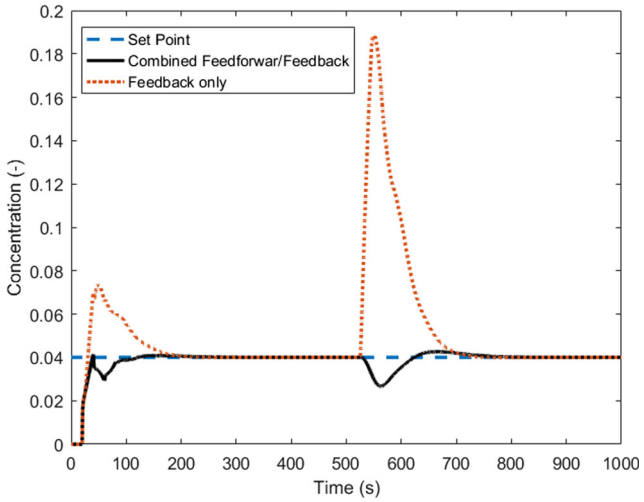

Fig. 28 Comparison of combined feedforward/feedback control with feedback-only control (step disturbance)

in the case of nonlinear actuator does not actuate the excipient feeder high enough and thus the total production rate before 500 s is less in the case of nonlinear actuator than in the case of linear actuator.

Evaluation of Combined Feedforward/Feedback Control (Nonlinear Actuator)

In order to implement a feedforward controller, the flowsheet was simplified and is described in Appendix A. This was done because during implementation, a combined transfer function model for the plant would be required and it also brings the model a step closer to implementation in the pilot plant. The simplified model was then simulated for feedback-only control strategy and for combined feedforward/feedback control strategy to compare the two responses.

Random Disturbance Rejection

A random disturbance was introduced in the API concentration at the outlet of the API feeder. Figure 26 shows the response for outlet concentration as a function of time under the feedback-only control strategy and the combined feedforward/feedback control strategy. As can be seen in the figure, the combined control strategy rejects the disturbance effectively while the feedback-only control strategy propagates the disturbance through the process. However, in practice the magnitude of the disturbances are not expected to that high and therefore, the feedback-only controller may be also sufficient. There is a comparatively high overshoot at startup for the feedback controller, however there is a slight undershoot for the combined control strategy. The rise time and settling time are less for both the controllers as is desired. Figure 27a shows the disturbance introduced to the process as a function of time. Figure 27b plots the actuator response (set point for the excipient feeder flow rate) as a function of time for the two control strategies. From this figure, it can be noted that the combined feedforward/feedback control reacts faster to the disturbance than feedback-only control. There are also higher magnitude oscillations in the actuator response for combined control, since it manipulates the actuator to a higher degree to maintain a constant concentration.

In Table 8, the time integral performance criteria are discussed. The root mean square error (RMSE) gives the standard deviation of the residuals and determines the average deviation of the response from the set point. As seen in

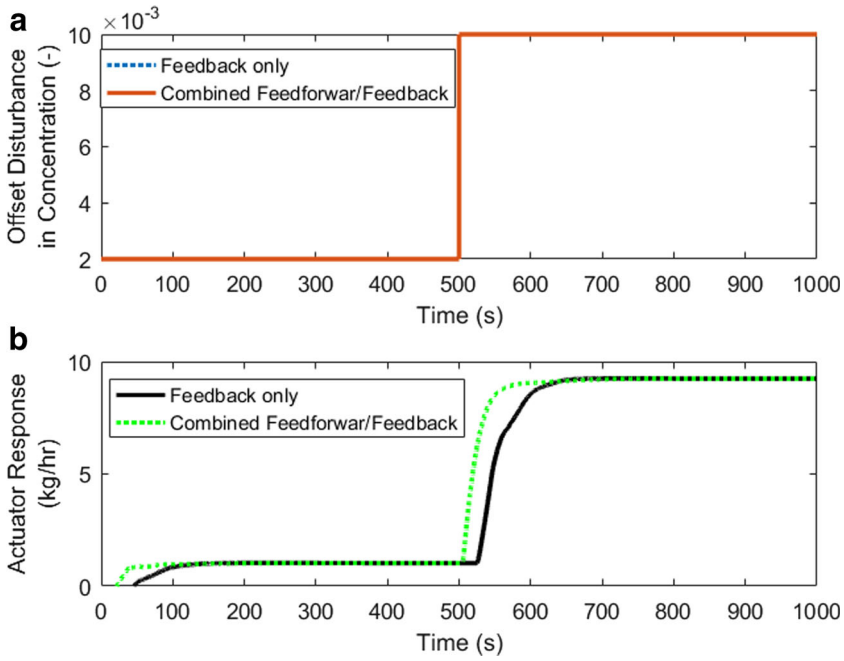

Fig. 29 **a** Disturbance (step) in concentration. **b** Actuator response, i.e., set point of excipient feeder flow rate (kg/h)

Table 9 Performance evaluation of combined feedforward/feedback control vs. feedback-only control (offset disturbance in concentration)

Controller	RMSE (−)	ITAE (−) s^2	ISE (−)^2 s	IAE (−) s	T2P (s)	D2R (s)	M2P (−)
Combined feedforward/feedback	0.0067	5863.755	0.284	19.046	31.4	163.7	−0.013
Feedback-only	0.0310	55,054.884	9.183	119.053	25.4	175.8	0.149

Table 8, a lower value of RMSE is obtained for the combined control strategy which is favorable. Integral time-weighted absolute error (ITAE) integrates the product of time and absolute error over time. When the ITAE tuning is applied, a quick settling response with smaller oscillations is obtained. However, the initial response is sluggish. The integral squared error (ISE) integrates the square of the error over time. Since the error is being squared, the ISE tuning will eliminate large errors quickly but will tolerate small errors. This will lead to a faster response having small consistent oscillations. Integral absolute error (IAE) integrates the absolute error over time. The IAE tuning results in slower response than the ISE but with fewer oscillations. Numerical values for these are given in Table 8 for random disturbance rejection. These values are smaller for the combined control strategy over the feedback-only strategy which indicates that the combined control strategy performs better and rejects disturbances more effectively.

Step Disturbance Rejection

A step disturbance was introduced in API concentration at the outlet of the API feeder. A step change of magnitude 10% was introduced to the concentration at 500 s. Figure 28 shows the response of the outlet concentration to the step disturbance as a function of time for the combined feedforward/feedback control strategy and the feedback-only control strategy. As seen in the figure, when the disturbance is introduced at 500 s, the feedback controller overshoots; however, the combined control strategy rejects this step disturbance and maintains the concentration approximately constant. Figure 29a shows the step change in the API concentration as a function of time. Figure 29b shows the actuator response to the step disturbance as a function of time for both the control strategies. The feedback-only control shows a delay in the actuator response when the disturbance was passed. However, the combined control strategy reacts faster to the disturbance by manipulating the set point for the excipient feeder flow rate.

Table 9 discusses the time integral performance criteria and some qualitative indicators for control performance of the two control strategies. The RMSE value for feedback-only control is about five times that for combined feedforward/feedback control which shows that the combined control strategy controls the concentration at the desired set point more effectively. The ITAE, ISE, and IAE values are also smaller for combined feedforward/feedback control in comparison to feedback-only control. Qualitative performance criteria have also been discussed for this disturbance rejection and these are time to product (T2P), duration to reject (D2R), and magnitude to product (M2P) [25]. T2P determines the time taken for the disturbance to affect the product from the time it first entered the process. From the values mentioned in Table 9, it takes longer for the disturbance to affect the product in the case of combined feedforward/feedback control. D2R gives the time taken for the disturbance to be rejected from when it first affected the product. This value is lower for the combined control strategy and thus it signifies that combined feedforward/feedback control rejects disturbances faster in comparison. M2P gives the maximum deviation from the set point after the disturbance has affected the product. For the combined feedforward/feedback controller,

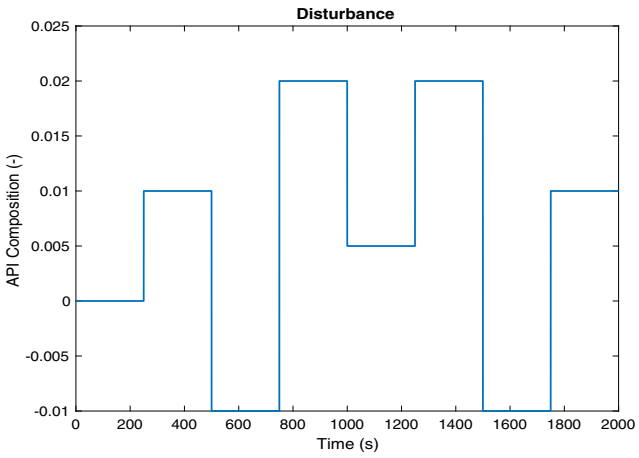

Fig. 30 Disturbance introduced (step changes in concentration)

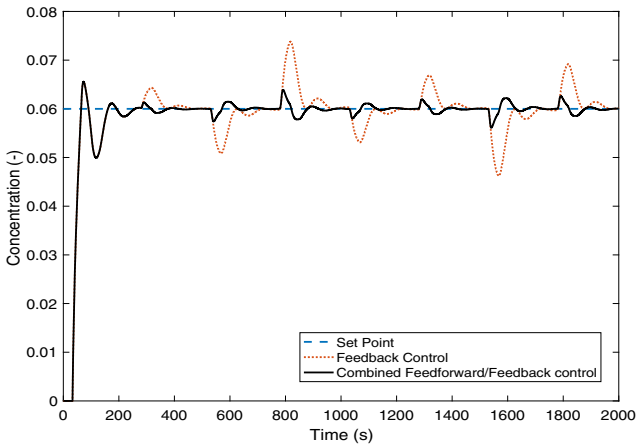

Fig. 31 Comparison of combined feedforward/feedback with feedback only for linear actuator

Table 10 Performance evaluation of combined feedforward/feedback control vs. feedback-only control (linear actuator)

Controller	RMSE (−)	ITAE (−) s^2	ISE (−)^2 s	IAE (−) s	T2P (s)	D2R (s)	M2P (−)
Combined feedforward/feedback	0.0086	11,895	1.1344	36.253	31.2	219.2	0.0013
Feedback-only	0.0093	43,032	1.3672	63.389	31.2	292.6	0.0046

there is a slight undershoot. However, for the feedback controller, the value is positive and shows a higher deviation in comparison to combined control strategy. Thus, from the two disturbance rejection analyses, it can be seen that under combined control strategy, the concentration of API is better controlled with no sustained oscillations.

Evaluation of Combined Feedforward/Feedback Control (Linear Actuator)

The "Evaluation of Combined Feedforward/Feedback Control (Nonlinear Actuator)" Section discusses the combined feedforward/feedback control strategy for the nonlinear actuator. This section focusses on evaluating the combined feedforward/feedback control strategy for the linear actuator. Offset types of disturbances were introduced in the concentration of API exiting the feeder since due to lack of blend uniformity, certain regions of the powder show either a higher concentration or a lower concentration. Figure 30 describes the disturbances introduced which are step changes every 250 s. The response of API composition in granules for feedback-only control and for combined feedforward/feedback control is described in Fig. 31. From the figure, it can be seen that every 250 s, when the disturbance is introduced, the feedback control has an overshoot or undershoot depending on the disturbance. However, in comparison to feedback only, combined feedforward/feedback control has lesser overshoot and settles comparatively faster.

Table 10 discusses the performance evaluation criteria and some qualitative indicators of the two control strategies for the linear actuator. The RMSE value for the combined control strategy is less than that for the feedback-only control strategy which shows that the combined control strategy controls the composition of API in granules more efficiently when an input

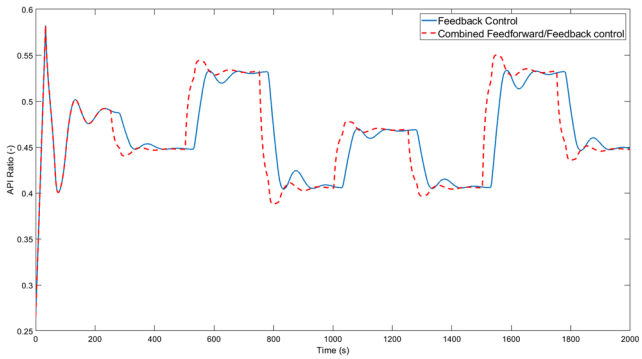

Fig. 32 Actuator response, i.e., API ratio

disturbance affects the process. From the table, we also see that the ITAE, ISE, and IAE values are smaller for the combined control strategy in comparison to the feedback-only control strategy. The T2P value for both the control strategies is the same which indicates that disturbance takes the same time to affect the product in both cases. The D2R value is smaller for combined control strategy than for feedback only which indicates that it rejects disturbances faster than feedback-only controller. The M2P value for feedback-only control is more than that for combined control as can also be seen in Fig. 31. Figure 32 shows the response of actuators under both control strategies.

Evaluation of MPC over PID Control (Linear Actuator)

In the "Evaluation of Combined Feedforward/Feedback Control (Nonlinear Actuator)" Section, a combined feedforward/feedback control was evaluated for the nonlinear actuator as one of the control options. In this section, the linear actuator-based transfer function model was used for PID control as well as model predictive control. The two control strategies were evaluated with a random disturbance in measurement.

Figure 33 is a comparison of the response for composition of API in granules for MPC as well as PID control. A random disturbance was added in the measured signal which is similar to that observed experimentally. The response for composition of API in granules for MPC is indicated in red dotted line while the response for composition of API in granules for

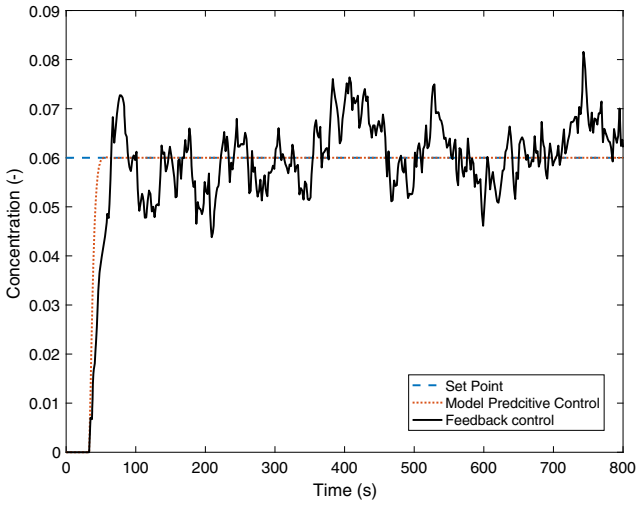

Fig. 33 Comparison of MPC with PID control for disturbance in measured signal

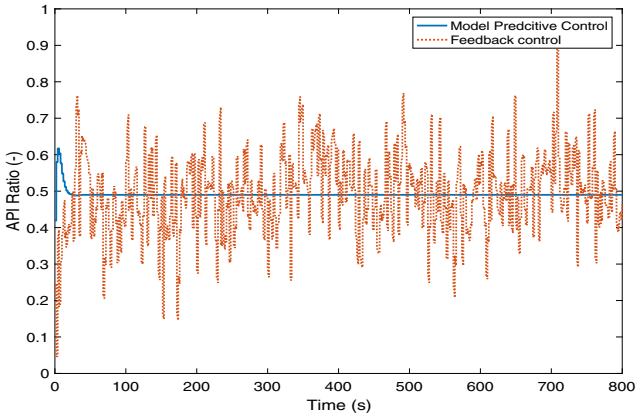

Fig. 34 Actuator response of MPC and PID control to disturbance in measured signal

PID control is indicated in black solid line. As can be seen, the rise time for MPC which is 54 s is less than that for PID control which is 65 s. It can also be clearly noted that MPC rejects the disturbance observed in the measured signal whereas PID controller does not reject it efficiently.

Figure 34 represents the actuator response to the disturbance in measured signal. The blue solid line indicates the actuator response for MPC control while the red dotted line indicates the actuator response for PID control. As can be seen, MPC does not actuate the API ratio as much as the PID controller does, since it accounts for the disturbance as the disturbance in measured signal and not process disturbance.

Table 11 gives the performance evaluation for MPC over PID control in the case of linear actuator. The RMSE value for

Table 11 Performance evaluation of MPC over PID control

Controller	RMSE (−)	ITAE (−) s^2	ISE (−)^2 s	IAE (−) s
Model predictive control	0.0127	418.6453	0.9482	17.0913
PID	0.0151	16,830.0000	1.4689	60.9941

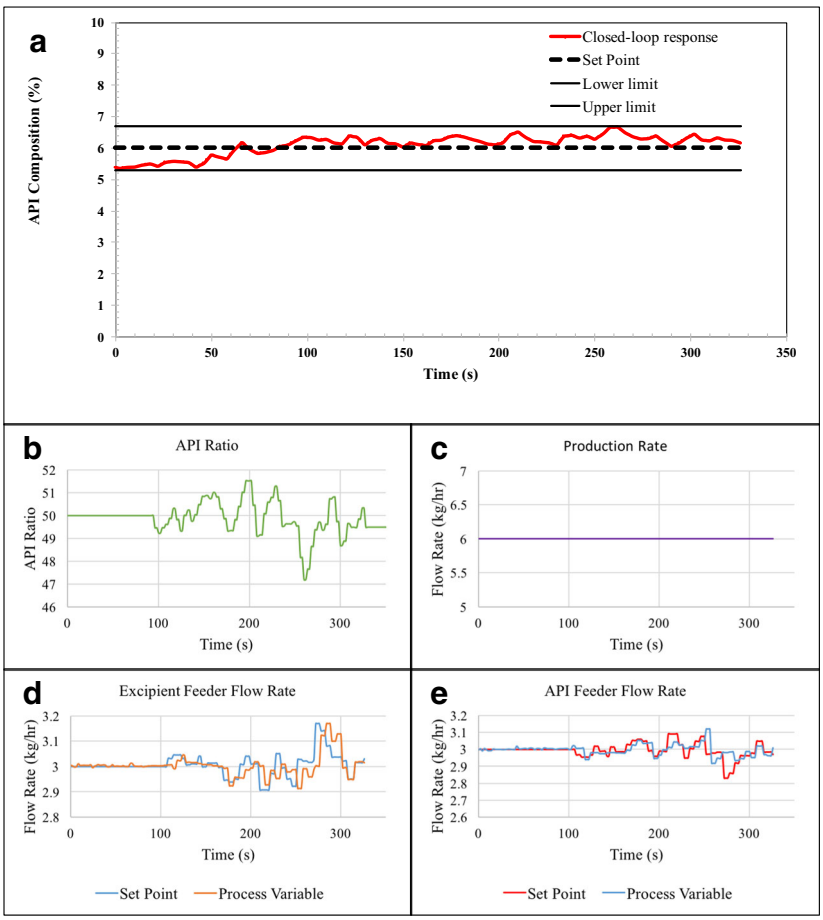

Fig. 35 **a** Implementation of feedback-based MPC controller in pilot plant. **b** Actuator–API ratio. **c** Total production flow rate. **d** Excipient-only feeder flow rate. **e** API + excipient feeder flow rate

MPC is less in comparison to feedback-only control which indicates that it controls the API composition in granules more efficiently and which can also be noticed in Fig. 33.

Implementation of Advanced Control in Pilot Plant

The control system was first evaluated in simulation mode before implementing it on the pilot plant. From the in silico study carried out in the previous sections, we see that model predictive control algorithm gives better performance and hence this control scheme was selected to be implemented on the pilot plant. The control platform integrated with the plant also provides for a model predictive controller. The developed MPC was then executed in real time in closed loop to test its efficiency. Two feeders were connected to the TSG, one consisting of API preblend and one consisting of excipient blend. A CDI NIR spectrometer (Wavelength Stable Back-Thinned 2D FFT CCD Array from Control Development Inc. Sound Bend, IN, USA) is used to measure the composition of API in granules at the outlet of the granulator. The developed PLS model is used to give real-time predictions for API composition in PharmaMV Real-Time system. These predictions are then used by the linear model generated for MPC which calculates the actuator following an algorithm and generates an actuator signal. The actuator signal is the API ratio which is sent to a ratio calculation block that calculates the flow rate set point of the two feeders.

Figure 35 shows the performance of the feedback-based MPC controller in the pilot plant. The control platform was initially running with the controller disabled. At 96 s, the controller was enabled. Figure 35a shows the API composition (%) in granules as measured by NIR. It should be noted that this is the filtered measurement where a moving average of 8 s was taken. During the time when the controller is active, the composition of API is controlled fairly efficiently to around 6% as can be seen from the figure. When the controller is not active, the composition of API is below 6% (before 96 s). Figure 35b shows the API ratio which is the manipulated variable. As seen in the figure, the manipulated variable changes when the controller is activated in order to control the composition of API in granules. As can be seen when the API ratio decreases, the API composition in granules increases and when the API ratio increases the API composition decreases. From the API ratio, the flow rate set point for the two feeders are calculated. Figure 35c shows the total production flow rate, which is held constant at 6 kg/h. Figure 35d and e shows the flow rates for the excipient feeder and the API blend feeder, respectively. Before 96 s, it can be seen that both the feeders operate at 3 kg/h. When the controller is activated, the flow rates change based on the change in API ratio. It can be seen from the figures that when the API composition is higher, the excipient feeder flow rate is increased while the API feeder flow rate is decreased bringing the API composition in granules to the set point value. Using the performance evaluation parameters discussed earlier, the controller performance is determined in comparison with the open loop process. The RMSE value when the controller is active is 0.31 compared to open loop which is 0.54. ITAE value is 3950, IAE is 30.9264, and ISE is 10.5197 for closed loop control while the respective values for open loop are 50897, 180.622, and 114.8573. Thus, a feedback-based MPC controller was successfully implemented with satisfactory control.

Conclusions

In this work, an advanced control strategy was developed for an integrated continuous granulation process and in silico study was performed. It is crucial to have pharmaceutical products of the right composition and thus it is important to develop control strategies around these unit operations. The unit operations considered in this process are the feeders and a continuous twin screw granulator. Control loops were designed around these two unit operations where the feeders consist of an inbuilt PID controller and a combined feedforward/feedback controller. The feedback controller considered is a PID and the feedforward controller was developed from the characteristic equation. The controllers were tested for set point tracking and disturbance rejection abilities for different types of disturbances. A comparison was made between the traditional feedback-only controller and a combined feedforward/feedback controller. The results show that the combined control strategy performs better in comparison to feedback-only control strategy. The feedforward controller rejects the disturbance before it affects the product while the feedback controller corrects process disturbances. It should be noted that the process model was assumed to be perfect and thus the controller model is ideal. A feedforward controller is specific to a particular process and material and thus it needs to be modified whenever there is a change in the process or the material. A comparison was also made between traditional PID controller and a model-based predictive (MPC) controller. The simulation study showed that MPC performs better in comparison to a PID controller. A feedback model predictive control system has been implemented in the experimental setup. For the manufacture of tablets, the process consists of other unit operations downstream from the granulator. Proposing a control strategy at this stage in the process is important since major disturbances are generated after the feeder unit operation. Thus, controlling at this stage avoids propagation of these disturbances further downstream. Future work includes implementation of the developed combined feedforward/feedback control strategy in an integrated continuous twin screw granulator process via a control platform.

Funding Information This work is supported by Glaxo Smith Kline (GSK) and the National Science Foundation Engineering Research Center on Structured Organic Particulate Systems, through Grant NSF-ECC 0540855.

Appendix

Feedforward Model

The feedforward controller model was developed in MATLAB workspace and Simulink. The integrated flowsheet model developed in gPROMS was converted to an integrated flowsheet model in Simulink. Transfer function models were developed from data generated by the gPROMS model. These models were developed in System Identification Toolbox and the best fit model was selected. The pole-zero plot and bode diagrams for these transfer functions were also developed to ensure that the transfer functions were stable. These transfer function models describe the various unit operations in the flowsheet. The flowsheet transfer function model is described in Fig. 36.

The above transfer function model was simplified because during implementation a simplified model for the entire process would be required. The simplified process model which also represents the ideal case was developed using the data generated by the Simulink model described in Fig. 36. The feedforward controller was then developed using the disturbance model and the process model given in Fig. 37. The feedforward controller transfer function is achieved by equating the characteristic equation to zero. The general form of that is given in Eq. 10. Both the disturbance transfer function (G_d) and process transfer function (G_p) are specific to a particular process and material and would change if any changes are made to the process or the materials.

$$G_{FF} = -\frac{G_d}{G_p} \tag{10}$$

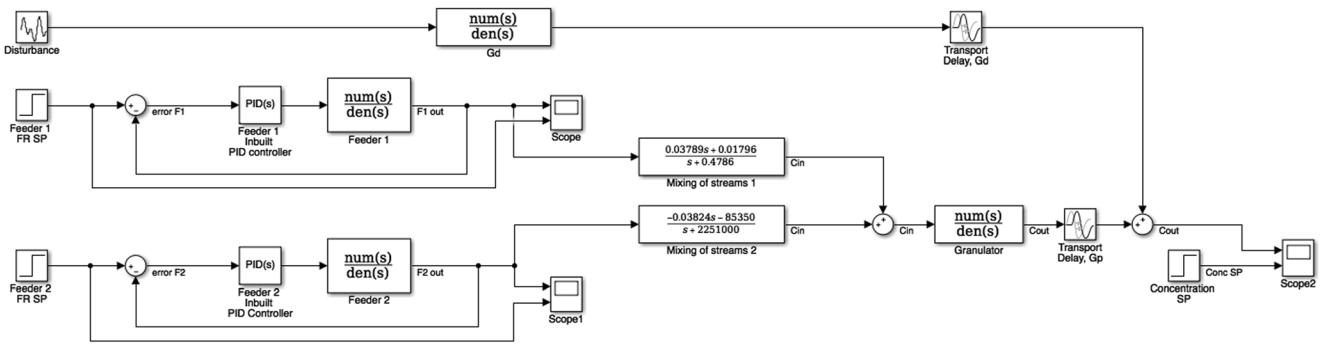

Fig 36 Integrated flowsheet model simulated in Simulink (open loop)

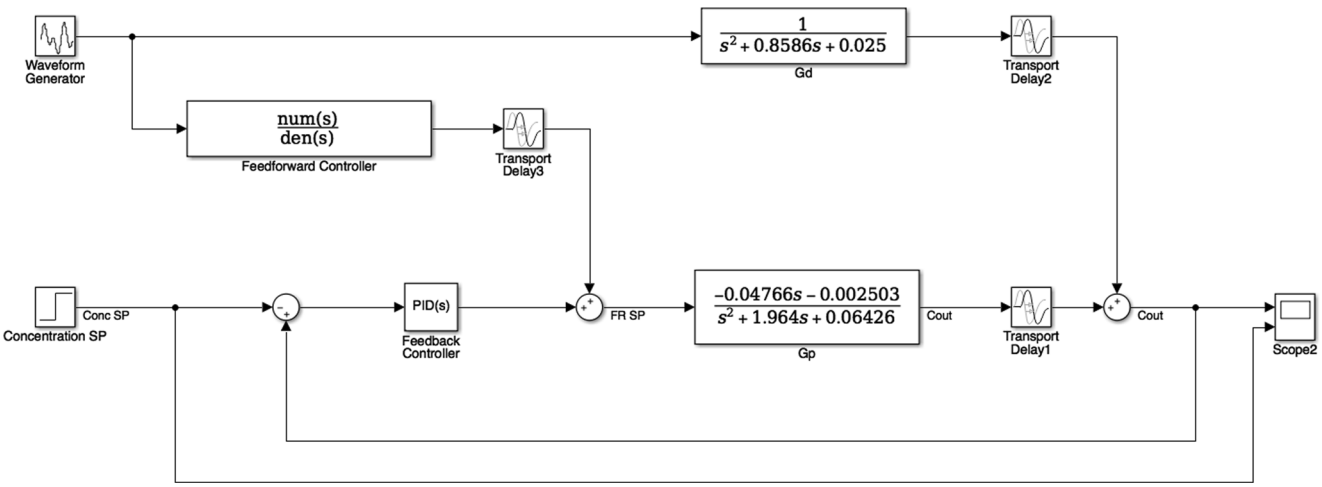

Fig. 37 Integrated flowsheet with combined feedforward/feedback control in Simulink

Appendix B: Nomenclature

Abbreviations	
APAP	Acetyl-para-aminophenol
API	Active pharmaceutical ingredient
CPM	Continuous pharmaceutical manufacturing
CPP	Critical process parameter
CQA	Critical quality attribute
CSTR	Continuously stirred tank reactor
CU	Content uniformity
D2R	Duration to reject
HPMC	Hypromellose
IAE	Integral of absolute error
ISE	Integral of square of error
ITAE	Integral of time absolute error
LOD	Loss on drying
L/S	Liquid to solid
M2P	Magnitude to product
MgSt	Magnesium stearate
MPC	Model predictive control
MRT	Mean residence time
MSC	Multiplicative scattering correction
NaStGly	Sodium starch glycolate
NIR	Near infrared
PAT	Process analytical technology
PFR	Plug flow reactor
PID	Proportional integral derivative
PLS	Partial least squares
QbD	Quality by design
RMSE	Root mean square error
RMSEP	Root mean square error of prediction
RSEP	Relative standard error of prediction
RSD	Relative standard deviation
RTD	Residence time distribution
SMCC	Silicified microcrystalline cellulose
SP	Set point
SSE	Sum of squared errors
T2P	Time to product
TSG	Twin screw granulator
WG	Wet granulation
Symbol	Variable
$G_d(s)$	Disturbance transfer function model
$G_p(s)$	Process transfer function model
G_c	Controller transfer function model
P	Proportional gain
I	Integral time constant
D	Derivative time constant
Subscript	Description
d	Disturbance
p	Process
c	Controller
1,2,3,4	Process or controller numbers

References

1. Schaber SD, Gergiorgis DI, Ramachandran R, Evans JMB, Barton PI, Trout BL. Economic analysis of integrated continuous and batch pharmaceutical manufacturing: a case study. Ind Eng Chem. 2011;50:10083–92. https://doi.org/10.1021/ie2006752.
2. Department of Health and Human Services. Pharmaceutical CGMPs for the 21st century—a risk based approach. United States Food and Drug Administration: Silver Spring, Maryland. 2004. https://www.fda.gov/downloads/Drugs/DevelopmentApprovalProcess/Manufacturing/QuestionsandAnswersonCurrentGoodManufacturingPracticescGMPforDrugs/UCM176374.pdf. Accessed 18 Aug 2016.
3. Department of Health and Human Services. Advancement of Emerging Technology Applications to Modernize the Pharmaceutical Manufacturing Base Guidance for Industry. United States Food and Drug Administration: Silver Spring, Maryland. 2015. https://www.fda.gov/downloads/Drugs/GuidanceComplianceRegulatoryInformation/Guidances/UCM478821.pdf. Accessed 18 Aug 2016.
4. Myerson AS, Krumme M, Nasr M, Thomas H, Braatz RD. Control systems engineering in continuous pharmaceutical manufacturing. May 20–21, 2014 continuous manufacturing symposium. J Pharm Sci. 2015;104:832–9. https://doi.org/10.1002/jps.24311.
5. Muteki K, Swaminathan V, Sekulic SS, Reid GL. Feed-forward process control strategy for pharmaceutical tablet manufacture using latent variable modeling and optimization technologies. IFAC Proceedings Volumes. 2012;45(15):51–6. https://doi.org/10.3182/20120710-4-SG-2026.00076.
6. Bardin M, Knight PC, Seville JPK. On control of particle size distribution in granulation using high-shear mixers. Powder Technol. 2004;140(3):169–75. https://doi.org/10.1016/j.powtec.2004.03.003.
7. Burggraeve A, Silva AFT, Kerkhof TVD, Hellings M, Vervaet C, Remon JP, et al. Development of a fluid bed granulation process control strategy based on real-time process and product measurements. Talanta. 2012;100:293–302. https://doi.org/10.1016/j.talanta.2012.07.054.
8. Sanders CFW, Hounslow MJ, Doyle FJ. Identification of models for control of wet granulation. Powder Technol. 2009;188(3):255–63. https://doi.org/10.1016/j.powtec.2008.05.005.
9. Singh R, Muzzio FJ, Ierapetritou M, Ramachandran R. A combined feed-forward/feed-back control system for a QbD-based continuous tablet manufacturing process. PRO. 2015;3(2):339–56. https://doi.org/10.3390/pr3020339.
10. Singh R, Velazquez C, Sahay A, Karry KM, Muzzio FJ, Ierapetritou MG, et al. Advanced control of continuous pharmaceutical tablet manufacturing processes. Process Simulation and Data Modeling in Solid Oral Drug Development and Manufacture. 2016:191–224. https://doi.org/10.1007/978-1-4939-2996-2_7.
11. Singh Ravendra BD, Chaudhary A, Sen M, Ierapetritou M, Ramachandran R. Closed-loop feedback control of a continuous pharmaceutical tablet manufacturing process via wet granulation. J Pharm Innov. 2014;9:16–37. https://doi.org/10.1007/s12247-014-9170-9.
12. Department of Health and Human Services. Guidance for Industry PAT-A Framework for Innovative Pharmaceutical Development, Manufacturing, and Quality Assurance. United States Food and Drug Administration: Silver Spring, Maryland. 2004. https://www.fda.gov/downloads/drugs/guidances/ucm070305.pdf . Accessed 09 Feb 2017.
13. Vanarase AU, Alcalà M, Jerez Rozo JI, Muzzio FJ, Romañach RJ. Real-time monitoring of drug concentration in a continuous powder

mixing process using NIR spectroscopy. Chem Eng Sci. 2010;65(21):5728–33. https://doi.org/10.1016/j.ces.2010.01.036.
14. Singh R, Sahay A, Karry KM, Muzzio F, Ierapetritou M, Ramachandran R. Implementation of an advanced hybrid MPC–PID control system using PAT tools into a direct compaction continuous pharmaceutical tablet manufacturing pilot plant. Int J Pharm. 2014;473(1):38–54. https://doi.org/10.1016/j.ijpharm.2014.06.045.
15. Singh R, Román-Ospino AD, Romañach RJ, Ierapetritou M, Ramachandran R. Real time monitoring of powder blend bulk density for coupled feed-forward/feed-back control of a continuous direct compaction tablet manufacturing process. Int J Pharm. 2015;495(1):612–25. https://doi.org/10.1016/j.ijpharm.2015.09.029.
16. Boukouvala F, Chaudhury A, Sen M, Zhou R, Mioduszewski L, Ierapetritou MG, et al. Computer-aided flowsheet simulation of a pharmaceutical tablet manufacturing process incorporating wet granulation. J Pharm Innov. 2013;8(1):11–27. https://doi.org/10.1007/s12247-012-9143-9.
17. Boukouvala F, Niotis V, Ramachandran R, Muzzio FJ, Ierapetritou MG. An integrated approach for dynamic flowsheet modeling and sensitivity analysis of a continuous tablet manufacturing process. Comput Chem Eng. 2012;42:30–47. https://doi.org/10.1016/j.compchemeng.2012.02.015.
18. Boukouvala F, Ramachandran R, Vanarase A, Muzzio FJ, Ierapetritou MG. Computer aided design and analysis of continuous pharmaceutical manufacturing processes. Computer Aided Chemical Engineering 201129;216–220; doi:https://doi.org/10.1016/B978-0-444-53711-9.50044-4, 2011.
19. Escotet-Espinoza M, Rogers A, Muzzio F, Ierapetritou M. Modeling of residence time distribution in continuous solid oral dose pharmaceutical manufacturing processes. AIChE annual meeting, Atlanta, GA. 20 2014.
20. Kumar A, Vercruysse J, Vanhoorne V, Toiviainen M, Panouillot PE, Juuti M, et al. Conceptual framework for model-based analysis of residence time distribution in twin-screw granulation. Eur J Pharm Sci. 2015;71:25–34. https://doi.org/10.1016/j.ejps.2015.02.004.
21. Marlin TE. Process control: designing processes and control systems for dynamic performance. 2nd ed. McGraw-Hill; 2000.
22. Coughanowr DR, LeBlanc SE. Process systems analysis and control. 3rd ed. McGraw-Hill Inc; 2009.
23. Román-Ospino AD, Singh R, Ierapetritou M, Ramachandran R, Méndez R, Ortega-Zuñiga C, et al. Near infrared spectroscopic calibration models for real time monitoring of powder density. Int J Pharm. 2016;512(1):61–74. https://doi.org/10.1016/j.ijpharm.2016.08.029.
24. Kremer DM, Hancock BC. Process simulation in the pharmaceutical industry: a review of some basic physical models. J Pharm Sci. 2006;95(3):517–29. https://doi.org/10.1002/jps.20583.
25. Haas NT, Ierapetritou M, Singh R. Advanced model predictive feedforward/feedback control of a tablet press. J Pharm Innov. 2017;12(2):110–23. https://doi.org/10.1007/s12247-017-9276-y.